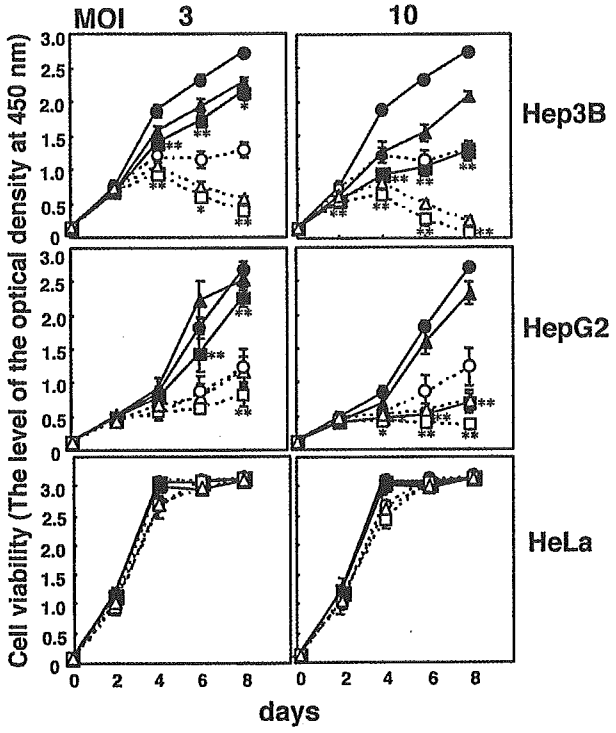

Figure 7. Additive inhibitory effects of Ad.RSV-HGF for cisplatin-treated hepatoma cells. Cell viability after infection with each Ad with or without cisplatin was determined by WST-8 assay. Although Ad.RSV-LacZ infection as well as Ad.RSV-HGF infection revealed additional inhibitory effects for HepG2 and Hep3B cells, but not for HeLa cells, additively to those of cisplatin, the degrees of the inhibitory effects were more prominent in the Ad.RSV-HGF-infected cells than those in the Ad.RSV-LacZ-infected ones. The open or closed symbols are indicated as the groups treated with or without cisplatin, respectively, while the circle, triangle and square symbols indicate no Ad-, Ad.RSV-LacZ- or Ad.RSV-HGF-treated groups, respectively. *P<0.05, **P<0.01 (Ad.RSV-LacZ groups versus Ad.RSV-HGF groups on each day at each MOI). N=8, each point in each group.

hepatomas might mean that the sequestration of Fas is lost by the c-Met and HGF-induced antiapoptotic effect in hepatomas. Although the identification of the molecules that were involved in these features were not the focus of the present study, overall elucidation in future studies may not only be of biological interest, but clinically useful for developing more effective HGF gene therapy.

On the other hand, the present study revealed clinically important information. The beneficial data obtained here may allow for the clinical application of adenoviral HGF gene therapy for CH and LC. First, high AGTE and the efficient expressions of exogenous HGF in an autocrine fashion in hepatomas may suggest that hepatomas are a good target site for gene transduction in the case of adenoviral HGF gene therapy for associated CH or LC; adenovirus-associated hepatotoxicity may be reduced. Second, the inhibitory effects of adenoviral HGF gene transduction for hepatomas, which resulted from not only the HGF-induced and Ad-induced inhibition of cell growth but also the HGF-induced apoptotic effects, are obviously encouraging for treating hepatoma itself. Another encouraging result was that Ad-induced and HGF-induced inhibitory effects were found to additively enhance (rather than diminish) cisplatin-induced cytotoxicity against hepatoma. Several mechanisms of the cisplatin-induced inhibitory effects have been reported, including cell cycle arrest by activating the CDK kinase inhibitor (49), and the induction of apoptosis by upregulating Fas and the Fas ligand (50,51). On the other hand, previous studies demonstrated that recombinant Ad induced cell cycle dysregulation by causing the inappropriate expression of cyclin proteins and down-regulation of E2F-1 independent of the Rb and p53 status (52,53). The present results suggest that each signal transduction pathway induced by cisplatin, adenovirus or HGF, including the unknown pathway mentioned above, may not directly cross-talk with each other. Thus, the additive and independent inhibitory effects of Ad, HGF and cisplatin against hepatomas may be clinically beneficial because HGF gene therapy may be not only applicable to, but also therapeutic for, hepatoma patients undergoing treatment with cisplatin.

To further verify such clinical implication, we tried to establish clinically-relevant animal models of orthotopic HCC and hepatoblastoma by transplanting Hep3B and HepG2 cells into severe combined immunodeficiency mice, however, high mortality and uncertain tumor formation were obstacles to further therapeutic experiments. On the other hand, the size of subcutaneously implanted tumor was slightly but insignificantly smaller in Ad.HGF-treated mice than that in Ad.LacZ-treated ones in our preliminary experiments (data not shown). However, we did not pursue these results because subcutaneous tumor models have sometimes led to rather misleading results due to the lack of tissue characteristics or native microenvironments (36,37). Likewise, current HCC-Tg models, in which multiple nodules of HCC appear without CH or LC on various schedules, are neither clinically relevant nor useful for assessing the clinical usefulness of gene therapy strategy (25). In this context, the clinically relevant animal model of HCC with LC or CH should be newly generated and the clinical usefulness of HGF gene therapy should be carefully investigated in future studies.

In conclusion, adenoviral HGF gene transduction in human hepatoblastomas and HCC inhibited their growth and induced apoptosis, as well as additively enhancing the cisplatin-induced inhibitory effect. These effects may be beneficial for HGF gene therapy for CH and LC associated with hepatomas.

Acknowledgements

This study was supported by a Grant-in-Aid for Scientific Research (C) from the Japan Society for the Promotion of Science. We thank Nippon Kayaku Co. Ltd. for providing cisplatin.

References

1. Nakamura T, Nawa K and Ichihara A: Partial purification and characterization of hepatocyte growth factor from serum of hepatectomized rats. Biochem Biophys Res Commun 122: 1450-1459, 1984.
2. Russell WE, McGowan JA and Bucher NL: Partial characterization of a hepatocyte growth factor from rat platelets. J Cell Physiol 119: 183-192, 1984.
3. Thaler FJ and Michalopoulos GK: Hepatopoietin A: partial characterization and trypsin activation of a hepatocyte growth factor. Cancer Res 45: 2545-2549, 1985.
4. Gohda E, Tsubouchi H, Nakayama H, Hirono S, Takahashi K, Koura M, Hashimoto S and Daikuhara Y: Human hepatocyte growth factor in plasma from patients with fulminant hepatic failure. Exp Cell Res 166: 139-150, 1986.

5. Nakamura T, Nishizawa T, Hagiya M, Seki T, Shimonishi M, Sugimura A, Tashiro K and Shimizu S: Molecular cloning and expression of human hepatocyte growth factor. Nature 342: 440-443, 1989.
6. Miyazawa K, Tsubouchi H, Naka D, Takahashi K, Okigaki M, Arakaki N, Nakayama H, Hirono S, Sakiyama O, *et al*: Molecular cloning and sequence analysis of cDNA for human hepatocyte growth factor. Biochem Biophys Res Commun 163: 967-973, 1989.
7. Matsumoto K and Nakamura T: Hepatocyte growth factor (HGF) as a tissue organizer for organogenesis and regeneration. Biochem Biophys Res Commun 239: 639-644, 1997.
8. Kosai K, Matsumoto K, Nagata S, Tsujimoto Y and Nakamura T: Abrogation of Fas-induced fulminant hepatic failure in mice by hepatocyte growth factor. Biochem Biophys Res Commun 244: 683-690, 1998.
9. Kosai K, Matsumoto K, Funakoshi H and Nakamura T: Hepatocyte growth factor prevents endotoxin-induced lethal hepatic failure in mice. Hepatology 30: 151-159, 1999.
10. Ueki T, Kaneda Y, Tsutsui H, Nakanishi K, Sawa Y, Morishita R, Matsumoto K, Nakamura T, Takahashi H, Okamoto E and Fujimoto J: Hepatocyte growth factor gene therapy of liver cirrhosis in rats. Nat Med 5: 226-230, 1999.
11. Matsuda Y, Matsumoto K, Ichida T and Nakamura T: Hepatocyte growth factor suppresses the onset of liver cirrhosis and abrogates lethal hepatic dysfunction in rats. J Biochem 118: 643-649, 1995.
12. Matsuda Y, Matsumoto K, Yamada A, Ichida T, Asakura H, Komoriya Y, Nishiyama E and Nakamura T: Preventive and therapeutic effects in rats of hepatocyte growth factor infusion on liver fibrosis/cirrhosis. Hepatology 26: 81-89, 1997.
13. Kosai KI, Finegold MJ, Thi-Huynh BT, Tewson M, Ou CN, Bowles N, Woo SL, Schwall RH and Darlington GJ: Retrovirus-mediated *in vivo* gene transfer in the replicating liver using recombinant hepatocyte growth factor without liver injury or partial hepatectomy. Hum Gene Ther 9: 1293-1301, 1998.
14. Jeffers M, Rong S and Woude GF: Hepatocyte growth factor/scatter factor-Met signaling in tumorigenicity and invasion/metastasis. J Mol Med 74: 505-513, 1996.
15. To CT and Tsao MS: The roles of hepatocyte growth factor/scatter factor and met receptor in human cancers (Review). Oncol Rep 5: 1013-1024, 1998.
16. Date K, Matsumoto K, Kuba K, Shimura H, Tanaka M and Nakamura T: Inhibition of tumor growth and invasion by a four-kringle antagonist (HGF/NK4) for hepatocyte growth factor. Oncogene 17: 3045-3054, 1998.
17. Kuba K, Matsumoto K, Date K, Shimura H, Tanaka M and Nakamura T: HGF/NK4, a four-kringle antagonist of hepatocyte growth factor, is an angiogenesis inhibitor that suppresses tumor growth and metastasis in mice. Cancer Res 60: 6737-6743, 2000.
18. Kan M, Zhang GH, Zarnegar R, Michalopoulos G, Myoken Y, McKeehan WL and Stevens JI: Hepatocyte growth factor/hepatopoietin A stimulates the growth of rat kidney proximal tubule epithelial cells (RPTE), rat nonparenchymal liver cells, human melanoma cells, mouse keratinocytes and stimulates anchorage-independent growth of SV-40 transformed RPTE. Biochem Biophys Res Commun 174: 331-337, 1991.
19. Tajima H, Matsumoto K and Nakamura T: Hepatocyte growth factor has potent anti-proliferative activity in various tumor cell lines. FEBS Lett 291: 229-232, 1991.
20. Shiota G, Rhoads DB, Wang TC, Nakamura T and Schmidt EV: Hepatocyte growth factor inhibits growth of hepatocellular carcinoma cells. Proc Natl Acad Sci USA 89: 373-377, 1992.
21. Miyazaki M, Gohda E, Tsuboi S, Tsubouchi H, Daikuhara Y, Namba M and Yamamoto I: Human hepatocyte growth factor stimulates the growth of HUH-6 clone 5 human hepatoblastoma cells. Cell Biol Int Rep 16: 145-154, 1992.
22. Tajima H, Matsumoto K and Nakamura T: Regulation of cell growth and motility by hepatocyte growth factor and receptor expression in various cell species. Exp Cell Res 202: 423-431, 1992.
23. Liu ML, Mars WM and Michalopoulos GK: Hepatocyte growth factor inhibits cell proliferation *in vivo* of rat hepatocellular carcinomas induced by diethylnitrosamine. Carcinogenesis 16: 841-843, 1995.
24. Shiota G, Wang TC, Nakamura T and Schmidt EV: Hepatocyte growth factor in transgenic mice: effects on hepatocyte growth, liver regeneration and gene expression. Hepatology 19: 962-972, 1994.
25. Sakata H, Takayama H, Sharp R, Rubin JS, Merlino G and La Rochelle WJ: Hepatocyte growth factor/scatter factor overexpression induces growth, abnormal development, and tumor formation in transgenic mouse livers. Cell Growth Differ 7: 1513-1523, 1996.
26. Takayama H, La Rochelle WJ, Sharp R, Otsuka T, Kriebel P, Anver M, Aaronson SA and Merlino G: Diverse tumorigenesis associated with aberrant development in mice overexpressing hepatocyte growth factor/scatter factor. Proc Natl Acad Sci USA 94: 701-706, 1997.
27. Shiota G, Kawasaki H, Nakamura T and Schmidt EV: Characterization of double transgenic mice expressing hepatocyte growth factor and transforming growth factor alpha. Res Commun Mol Pathol Pharmacol 90: 17-24, 1995.
28. Santoni-Rugiu E, Preisegger KH, Kiss A, Audolfsson T, Shiota G, Schmidt EV and Thorgeirsson SS: Inhibition of neoplastic development in the liver by hepatocyte growth factor in a transgenic mouse model. Proc Natl Acad Sci USA 93: 9577-9582, 1996.
29. Tsukada Y, Miyazawa K and Kitamura N: High intensity ERK signal mediates hepatocyte growth factor-induced proliferation inhibition of the human hepatocellular carcinoma cell line HepG2. J Biol Chem 276: 40968-40976, 2001.
30. Monto A and Wright TL: The epidemiology and prevention of hepatocellular carcinoma. Semin Oncol 28: 441-449, 2001.
31. Seeff LB: Natural history of chronic hepatitis C. Hepatology 36: S35-S46, 2002.
32. Romeo R and Colombo M: The natural history of hepatocellular carcinoma. Toxicology 181-182: 39-42, 2002.
33. Chen SH, Chen XH, Wang Y, Kosai K, Finegold MJ, Rich SS and Woo SL: Combination gene therapy for liver metastasis of colon carcinoma *in vivo*. Proc Natl Acad Sci USA 92: 2577-2581, 1995.
34. Chen SH, Kosai K, Xu B, Pham-Nguyen K, Contant C, Finegold MJ and Woo SL: Combination suicide and cytokine gene therapy for hepatic metastases of colon carcinoma: sustained antitumor immunity prolongs animal survival. Cancer Res 56: 3758-3762, 1996.
35. Caruso M, Pham-Nguyen K, Kwong YL, Xu B, Kosai KI, Finegold M, Woo SL and Chen SH: Adenovirus-mediated interleukin-12 gene therapy for metastatic colon carcinoma. Proc Natl Acad Sci USA 93: 11302-11306, 1996.
36. Terazaki Y, Yano S, Yuge K, Nagano S, Fukunaga M, Guo ZS, Komiya S, Shirouzu K and Kosai K: An optimal therapeutic expression level is crucial for suicide gene therapy for hepatic metastatic cancer in mice. Hepatology 37: 155-163, 2003.
37. Fukunaga M, Takamori S, Hayashi A, Shirouzu K and Kosai K: Adenoviral herpes simplex virus thymidine kinase gene therapy in an orthotopic lung cancer model. Ann Thorac Surg 73: 1740-1746, 2002.
38. Nagano S, Yuge K, Fukunaga M, Terazaki Y, Fujiwara H, Komiya S and Kosai K: Gene therapy eradicating distant disseminated micro-metastases by optimal cytokine expression in the primary lesion only: novel concepts for successful cytokine gene therapy. Int J Oncol 24: 549-558, 2004.
39. Matsumoto K, Kataoka H, Date K and Nakamura T: Cooperative interaction between alpha- and beta-chains of hepatocyte growth factor on c-Met receptor confers ligand-induced receptor tyrosine phosphorylation and multiple biological responses. J Biol Chem 273: 22913-22920, 1998.
40. Enari M, Sakahira H, Yokoyama H, Okawa K, Iwamatsu A and Nagata S: A caspase-activated DNase that degrades DNA during apoptosis, and its inhibitor ICAD. Nature 391: 43-50, 1998.
41. Sahara S, Aoto M, Eguchi Y, Imamoto N, Yoneda Y and Tsujimoto Y: Acinus is a caspase-3-activated protein required for apoptotic chromatin condensation. Nature 401: 168-173, 1999.
42. Llovet JM and Bruix J: Systematic review of randomized trials for unresectable hepatocellular carcinoma: chemoembolization improves survival. Hepatology 37: 429-442, 2003.
43. Schwartz JD and Beutler AS: Therapy for unresectable hepatocellular carcinoma: review of the randomized clinical trials-II: systemic and local non-embolization-based therapies in unresectable and advanced hepatocellular carcinoma. Anticancer Drugs 15: 439-452, 2004.
44. Shima N, Stolz DB, Miyazaki M, Gohda E, Higashio K and Michalopoulos GK: Possible involvement of p21/waf1 in the growth inhibition of HepG2 cells induced by hepatocyte growth factor. J Cell Physiol 177: 130-136, 1998.

45. Zhang H, Ozaki I, Mizuta T, Yoshimura T, Matsuhashi S, Hisatomi A, Tadano J, Sakai T and Yamamoto K: Mechanism of beta 1-integrin-mediated hepatoma cell growth involves p27 and S-phase kinase-associated protein 2. Hepatology 38: 305-313, 2003.
46. Wang X, De Frances MC, Dai Y, Pediaditakis P, Johnson C, Bell A, Michalopoulos GK and Zarnegar R: A mechanism of cell survival: sequestration of Fas by the HGF receptor Met. Mol Cell 9: 411-421, 2002.
47. Nagao M, Nakajima Y, Hisanaga M, Kayagaki N, Kanehiro H, Aomatsu Y, Ko S, Yagita H, Yamada T, Okumura K and Nakano H: The alteration of Fas receptor and ligand system in hepatocellular carcinomas: how do hepatoma cells escape from the host immune surveillance *in vivo*? Hepatology 30: 413-421, 1999.
48. Lee SH, Shin MS, Lee HS, Bae JH, Lee HK, Kim HS, Kim SY, Jang JJ, Joo M and Kang YK: Expression of Fas and Fas-related molecules in human hepatocellular carcinoma. Hum Pathol 32: 250-256, 2001.
49. Nishio K, Fujiwara Y, Miyahara Y, Takeda Y, Ohira T, Kubota N, Ohta S, Funayama Y, Ogasawara H, Ohata M, *et al*: Cis-diamminedichloroplatinum(II) inhibits p34cdc2 protein kinase in human lung-cancer cells. Int J Cancer 55: 616-622, 1993.
50. Muller M, Strand S, Hug H, Heinemann EM, Walczak H, Hofmann WJ, Stremmel W, Krammer PH and Galle PR: Drug-induced apoptosis in hepatoma cells is mediated by the CD95 (APO-1/Fas) receptor/ligand system and involves activation of wild-type p53. J Clin Invest 99: 403-413, 1997.
51. Muller M, Wilder S, Bannasch D, Israeli D, Lehlbach K, Li-Weber M, Friedman SL, Galle PR, Stremmel W, Oren M and Krammer PH: p53 activates the CD95 (APO-1/Fas) gene in response to DNA damage by anticancer drugs. J Exp Med 188: 2033-2045, 1998.
52. Wersto RP, Rosenthal ER, Seth PK, Eissa NT and Donahue RE: Recombinant, replication-defective adenovirus gene transfer vectors induce cell cycle dysregulation and inappropriate expression of cyclin proteins. J Virol 72: 9491-9502, 1998.
53. Kuhn H, Liebers U, Gessner C, Karawajew L, Ruppert V, Schumacher A, Witt C and Wolff G: Infection of cells with replication deficient adenovirus induces cell cycle alterations and leads to downregulation of E2F-1. Biochim Biophys Acta (BBA) - Mol Cell Res 1542: 106-115, 2002.

Diffuse encephaloventriculitis and substantial leukoencephalopathy after intraventricular administration of recombinant adenovirus

Tsuyoshi Tada*, John Bang Nguyen†, Yasuyuki Hitoshi†, Nathan P. Watson†, Jeffrey F. Dunn‡, Shinji Ohara§, Satoshi Nagano¶, Ken-ichiro Kosai¶ and Mark A. Israel†

*Department of Neurosurgery Shinshu University School of Medicine, Asahi 3-1-1, Matsumoto 390-8621, Japan
†Israel Laboratory, NCCC Research, Norris Cotton Cancer Center, Dartmouth Medical School, Hanover NH 03755, USA
‡Biomedical NMR Laboratory, Department of Diagnostic Radiology, Dartmouth Medical School, HB 7786, Hanover NH 03755, USA
§Department of Neurology, National Chushin Matsumoto Hospital, Kotobuki 811, Matsumoto 390-0021, Japan
¶Division of Gene Therapy and Regenerative Medicine, Cognitive and Molecular Research Institute of Brain Diseases, Kurume University, Asahi-machi 67, Kurume 830-0011, Japan

Objectives: *The use of recombinant adenovirus as a vehicle for gene transfer into ependymal cells is a potential therapeutic tool for the treatment of various neural disorders. However, gene transfer into the ependymal cells of the ventricular wall is associated with high-level expression of the transferred gene, which declines rapidly. The purpose of this study is to understand the cause of this early decline in gene expression.*

Methods: *Different doses of adenovirus-expressing β-galactosidase (Ad-β-gal) were injected into the lateral brain ventricle of C57BL/6 mice, and the brains were observed histologically and with magnetic resonance (MR) imaging for a month.*

Results: *Inoculation of the lateral ventricle with more than 1×10^8 viral particles (2.6×10^6 pfu) resulted in a rapid decline of β-gal expression. MR imaging indicated gradual ventriculomegaly and histological analysis showed the loss of the ependymal cells from the ventricular wall, lymphocytes infiltration near the wall, degeneration of myelinated fibers and apoptosis in the external capsule. Reactive astrocytes proliferated in the external capsule 17 days following inoculation. To avoid this irreversible brain atrophy, the inoculated adenovirus should be reduced to less than 1×10^7 particles (2.6×10^5 pfu) in mice.*

Discussion: *Our results indicate the presence of a unique and diffuse immune response of the brain; therefore, the clinical use of recombinant virus for intraventricular gene transfer must be carefully evaluated.* [Neurol Res 2005; **27**: 378–386]

Keywords: Adenovirus; encephaloventriculitis; leukoencephalopathy; mouse; ventricles

INTRODUCTION

Because systematically administrated bioactive substances cannot efficiently pass the blood–brain barrier[1], therapeutic proteins and peptides must be delivered directly in the central nervous system (CNS) for the treatment of neural disorders such as subarachnoid dissemination of malignant tumors and ischemic disorders[2–4].

The ependymal cell is an ideal target for gene therapy because gene products released into the cerebrospinal fluid (CSF) may access various cells in the CNS through the Virchow–Robbins spaces[5–7].

Recombinant adenovirus provides a suitable vehicle for gene transfer into cells of the CNS, because of its ability to efficiently deliver genes into non-replicating cells[8,9]. Almost all trans-gene experiments targeting ependymal cells have used recombinant adenovirus as vehicles for gene transfer[10–20]. However, despite favorable results in animal models, the efficacy of intraventricular administration of recombinant virus has not yet been proven in human studies[21,22]. Viral inoculation immediately stimulates both the humoral and cellular immune response of the host. This immune response has been shown to be a determining factor for the duration of the gene expression[23,24]. In the liver, expression of transferred genes declines rapidly; however, gene transfer into the brain has been reported to result in long-term expression[8,25,26]. Therefore, the brain has often been regarded as an organ that is protected from immune reactions. To realize the clinical

Correspondence and reprint requests to: [tadatsu@hsp.md.shinshu-u.ac.jp] Accepted for publication December 2004.

10.1179/016164105X22075

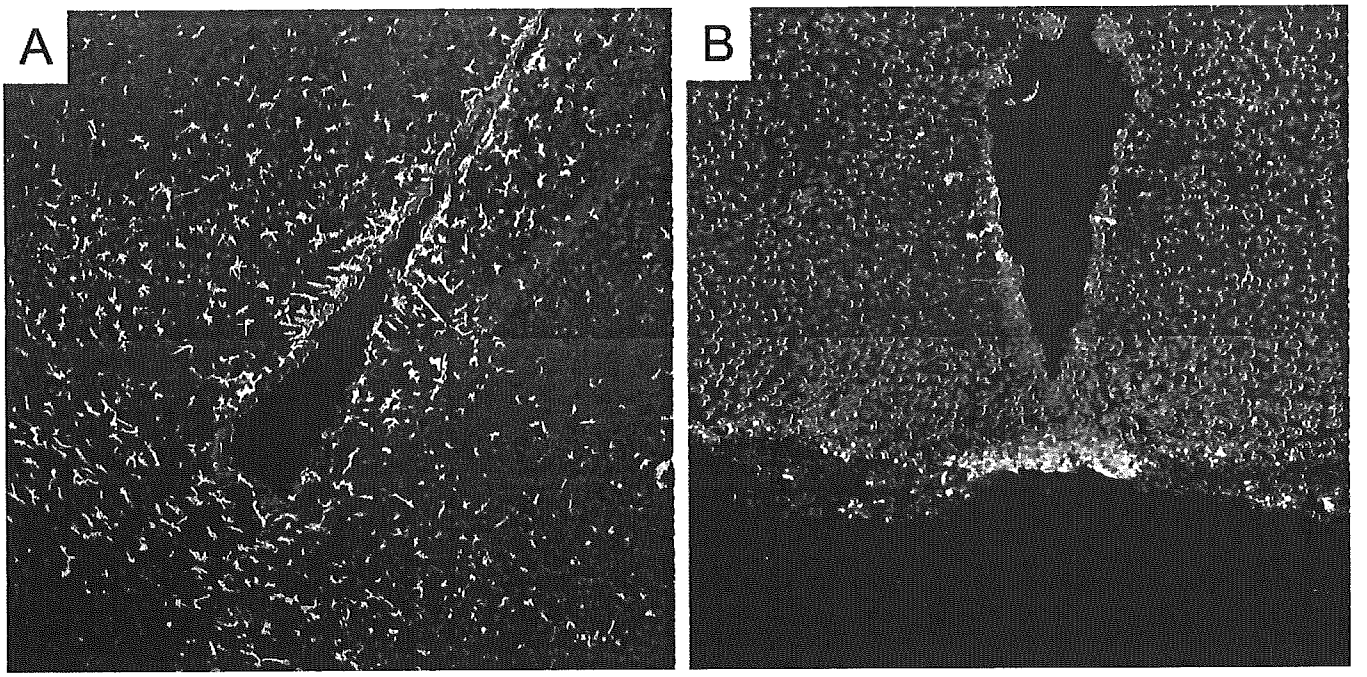

Figure 1: Expression of β-gal in the ependymal layer lining the third ventricle after the inoculation of 1×10^9 particles (2.6×10^7 pfu) of adenovirus. (A) The brain 4 days after inoculation. The section was incubated with rabbit anti-β-gal antibody, and goat anti-GFAP antibody. The secondary antibodies used were FITC-conjugated anti-rabbit antibody and RR-conjugated anti-goat antibody. RR-positive cells indicate ependymal cells. (B) The brain 7 days after the inoculation. The section was treated with rabbit anti-β-gal antibody and FITC-conjugated anti-rabbit antibody. Only a few β-gal-positive cells remain in the third ventricular wall

application of intraventricular gene therapy, we should more carefully examine the inflammatory and immune response of the host after the virus inoculation in the CNS[27,28].

In this study, we examined the cause of the early decline of gene expression from the ventricular wall. Magnetic resonance (MR) imaging and histological observations indicated an immune response following viral inoculation of both the brain parenchyma and the ventricular wall. However, the immune response in the ventricle was much more severe and was associated with diffuse encephalo-ventriculitis and substantial brain atrophy.

MATERIALS AND METHODS

Animals and reagents

C57BL/6 mice were purchased from Charles River Laboratories (Wilmington, MA). These mice were housed in a polycarbonate cage in the Animal Care Facility at the Dartmouth School of Medicine, and were fed with a commercial diet (LM-485 Mouse/Rat sterilizable diet 7012, Madison, WI). All mice were kept under a 12:12 hour dark–light cycle (lights turned on at 09:00). The room was kept at 24 ± 2°C and at 55 ± 10% relative humidity. Animal care was conducted in accordance with the 'Principles of Laboratory Animal Care' formulated by the National Society for Medical Research[29] and the 'Guide for the Care and Use of Laboratory Animals' prepared by the National Academy of Sciences and published by the National Institutes of Health (NIH Publication No. 86-23, revised 1996)[30].

Recombinant adenoviral vectors

E1 and E3 deleted adenoviral vector encoding β-galactosidase (Ad-β-gal) was prepared as described by Mizuguchi and Kay[32].

Anesthesia

Mice were sedated by intraperitoneal injection of a mixture of ketamine hydrochloride (2.5 mg/mouse) and medetomidine (0.025 mg/mouse). To reverse the anesthesia, antipamezole hydrochloride (0.125 mg/mouse) was injected[33].

Stereotaxic surgery

Once sedated, mice were placed in a stereotaxic frame (Model 900, Pembroke Pines, FL). A hole was made in the skull, 0.6 mm caudal from the coronal suture and 1 mm lateral from the midline. Ad-β-gal (1×10^9, 1×10^8, 1×10^7 particles/10 μl/mouse) was injected at a depth of 4 mm with a 10 μl Hamilton syringe on day 0.

MR imaging

Mouse brains were examined on days 3, 8, 17 and 29 with 7.0-tesla whole-body MR imaging. Others were killed after MR imaging. T2-weighted images were obtained with sequences (coronal plane; slice, 0.5 cm; TE, 90 milliseconds; TR, 2000 milliseconds).

Histological procedures

Deeply sedated mice were perfused with cold 4% paraformaldehyde (Electron Microscopy Sciences,

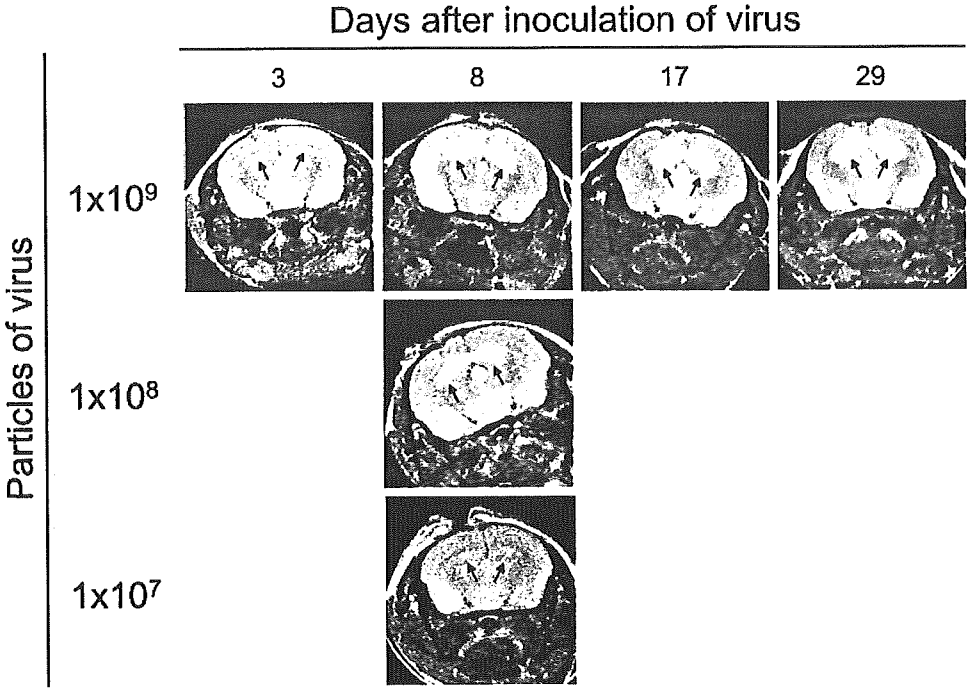

Figure 2: MR images taken at days 3, 8, 17 and 29 following the inoculation of 1×10^9 particles (2.6×10^7 pfu) of adenovirus encoding β-gal, and 8 days after the inoculation of 1×10^8 or 1×10^7 viral particles. The images taken 3 days after the inoculation of 1×10^9 particles as well as 8 days after the inoculation of 1×10^7 particles of the virus were consistent with a normal brain. The images taken 8 days after the inoculation of 1×10^9 and 1×10^8 viral particles showed mild ventriculomegaly. The ventricular system gradually dilated between days 17 and 29. Arrows indicate lateral ventricles

Hatfield, PA) in 0.1% phosphate-buffered saline, pH 7.4. One-half of the brain was dehydrated with a gradient sucrose solution, and was frozen at −80°C. The other half was embedded in paraffin.

The frozen brain was cut in 20 μm sections, and the sections were incubated with rabbit polyclonal anti-β-gal antibody (1:5000), IgG fraction (Cortex Biochem, San Leandro, CA) or goat polyclonal anti-glial fibrillary acidic protein (GFAP) antibody (1:5000). Fluorescein isothiocyanate (FITC)-conjugated horse anti-rabbit antibody or rhodamin red (RR)-conjugated horse anti-goat antibody (Jackson Immuno Research Laboratories, West Grove, PA) were used as secondary antibodies. Specimens were mounted in VECTASHIELD mounting medium with DAPI (Vector, Burlingame, CA).

Paraffin-embedded brains were cut in to 4 μm sections and stained with HE. Immunohistochemical studies were performed on the paraffin-embedded sections using the avidin–biotin–peroxidase complex (ABC) method with a Vectastain ABC kit (Vector, Burlingame, CA). The primary antibodies specific for apoptotic cells, myelin basic protein (MBP) and GFAP were polyclonal rabbit anti-single stranded DNA antibody (1:100) (DakoCytomation Co. Ltd, Kyoto, Japan), polyclonal rabbit anti-human MBP (1:1) (DakoCytomation), rabbit anti-Cow GFAP (1:500) (DakoCytomation), respectively.

RESULTS

Gene transfer to ependymal cells

Four days after the inoculation of 1×10^9 viral particles (2.6×10^7 pfu) in the lateral ventricle wall, double-staining with anti-GFAP and anti-β-gal antibodies shows the presence of a single layer of β-gal-positive cells in the third ventricular wall (*Figure 1A*). These β-gal-positive cells did not co-stain with the GFAP antibody. Seven days after the inoculation of 1×10^9 particles (2.6×10^7 pfu), staining with an FITC-conjugated anti-β-gal antibody shows a reduction in the number of β-gal-positive cells, and only a few positive cells were observed in the third ventricular wall and the parenchyma (*Figure 1B*).

MR follow-up after intraventricular inoculation of virus

MR imaging of the brains at day 3 following intraventricular inoculation of 1×10^9 particles (2.6×10^7 pfu) showed no brain abnormalities (*Figure 2*). Similarly, MR images taken at day 8 following inoculation of 1×10^7 particles (1×10^5 pfu) were consistent with a normal brain. In contrast, the MR images taken 8 days after the inoculation of 1×10^9 and 1×10^8 particles showed mild ventriculomegaly, and the ventricular system appeared more dilated at days 17 and 29.

HE staining of the brain after intraventricular inoculation of the virus

Intraventricular inoculation of more than 1×10^8 viral particles resulted in the infiltration of mononuclear cells into the ventricular wall and perivascular space, and the concomitant loss of ependymal cells from the ventricular wall (*Figure 3*).

Figure 4 shows HE staining of the external capsule at days 8, 17 and 29 days following inoculation of 1×10^9

Figure 3: HE staining of the paraventricular portion of the lateral ventricle and the third ventricle 8 days following inoculation of 1×10^8 particles (2.6×10^6 pfu) (A and B) or 1×10^7 particles (2.6×10^5 pfu) (C and D) of adenovirus encoding β-gal, respectively. The infiltration of mononuclear cells into the ventricular wall and perivascular space, and loss of ependymal cells from the ventricular wall was apparent after the inoculation of 1×10^9 viral particles. Bar=100 μm

particles (2.6×10^7 pfu) and 1×10^7 particles (2.6×10^5 pfu), respectively. An edematous change is clearly apparent in the external capsule following inoculation with the higher dose of 1×10^9 particles (2.6×10^7 pfu).

Analysis at a higher resolution reveals a microcystic change in the tissue surrounding the external capsule following the inoculation of 1×10^9 viral particles. In addition, proliferation of cells with large, clear nuclei was observed in the external capsule at days 17 and 29. These phenomena were not observed following the intraventricular inoculation with the lower dose of 1×10^7 particles (*Figure 5*).

Immunostaining of the brain after intraventricular administration of the virus

To estimate the proliferation of cells having large clear cells in the external capsule in HE staining, we examined them immunohistologically. Immunostaining for MBP showed a decrease in myelinated fibers as well as fragmentation of these fibers in the external capsule following the inoculation of 1×10^8 viral particles. A decrease and fragmentation of myelinated fibers did not occur following inoculation with the lower dose of 1×10^8 viral particles (*Figure 6*).

Inoculation of 1×10^9 particles resulted in significant apoptosis in the bilateral external capsule by day 8 (*Figure 7*), but only a few apoptotic cells were observed at days 17 and 29. Inoculation of 1×10^7 particles did not result in apoptosis by day 8 (data not shown).

The cytoplasm of the cells having a large clear nucleus proliferated in the external capsule at 17 and 29 days following inoculation of the virus was positive for anti-GFAP antibody (*Figure 8*)

DISCUSSION

When recombinant adenovirus is inoculated into the brain parenchyma, $CD4^+$ and $CD8^+$ T cells, and macrophages soon accumulate and MHC I is up-regulated in the vascular endothelium within 24 hours[24,34]. Because the immune response is also elicited by adenovirus that does not express β-gal, as well as ultraviolet-irradiated virus, the virus particles by themselves can induce inflammation at the injection site (our personal data)[34]. Despite the immune response, the expression of the transferred gene is apparent by the next day and numerous positive cells are seen after 60 days in the rat brain parenchyma[34]. Interestingly, the duration of gene expression is substantially longer in the brain than in other organs[25]. For example, Davidson *et al.* inoculated 5×10^7 pfu of Ad-β-gal into the mouse caudate putamen, and the gene expression continued for at least 8 weeks[26]. This long-term expression is generally explained by the observation that immune responses are typically less strong in the brain when compared with other organs[35]. Lowenstein described that up to 1×10^8 pfu of adenoviral vectors

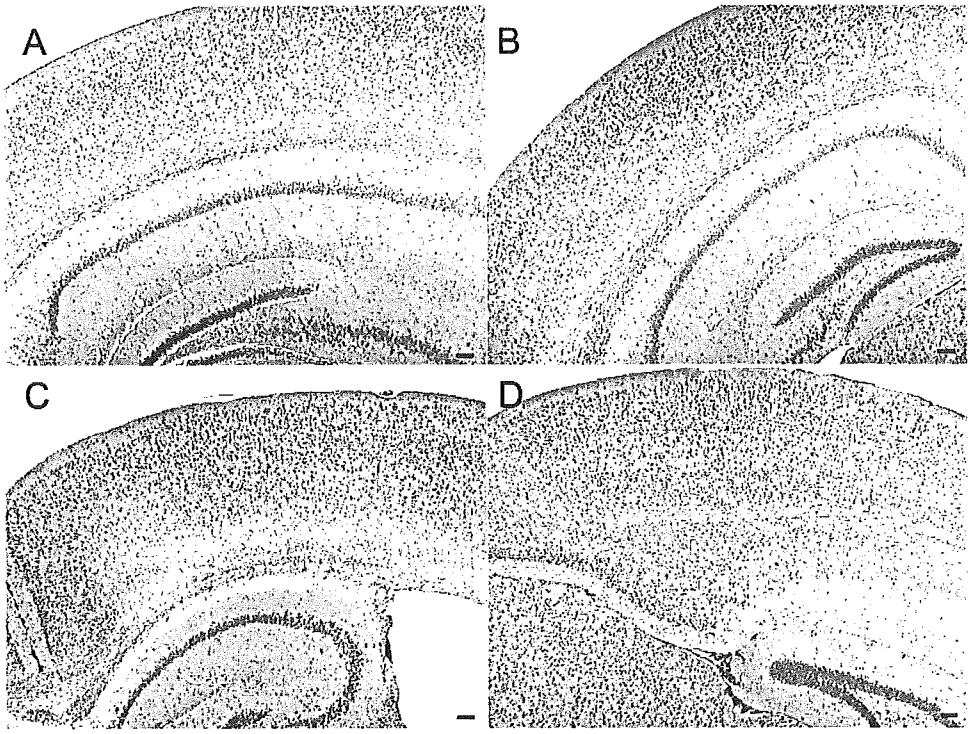

Figure 4: HE staining of the external capsule of the brains at days 8 (A), 17 (B) and 29 (C) following inoculation of 1×10^9 particles (2.6×10^7 pfu), or 1×10^7 of adenovirus encoding β-gal (2.6×10^5 pfu) (D). The edematous change was apparent near the external capsule of the brains at days 8, 17 and 29 following inoculation of 1×10^9 viral particles. Bar=100 μm

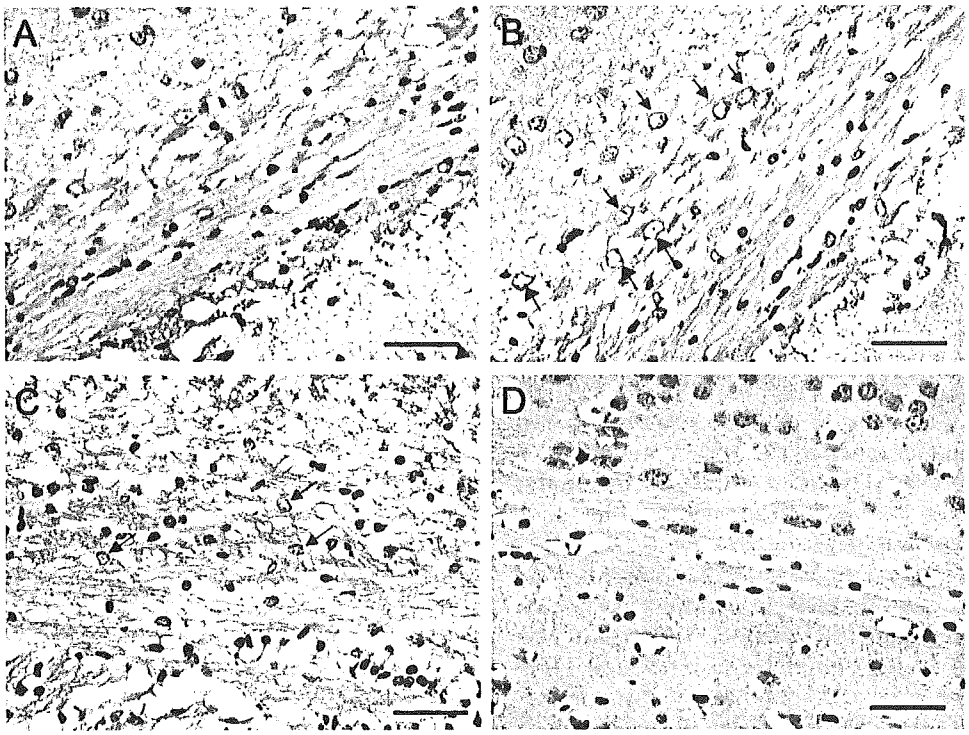

Figure 5: HE staining of the external capsule of the brain at days 8 (A), 17 (B) and 29 (C) following inoculation of 1×10^9 particles (2.6×10^7 pfu), or 1×10^7 of adenovirus encoding β-gal (2.6×10^5 pfu) (D). Microcystic change is apparent in the tissue surrounding the external capsule of the brains at days 8, 17 and 29 following inoculation of 1×10^9 viral particles. Many cells characterized by large clear nuclei proliferated into the external capsule of the brains 17 and 29 days after the inoculation of 1×10^9 viral particles (arrow). Bar=50 μm

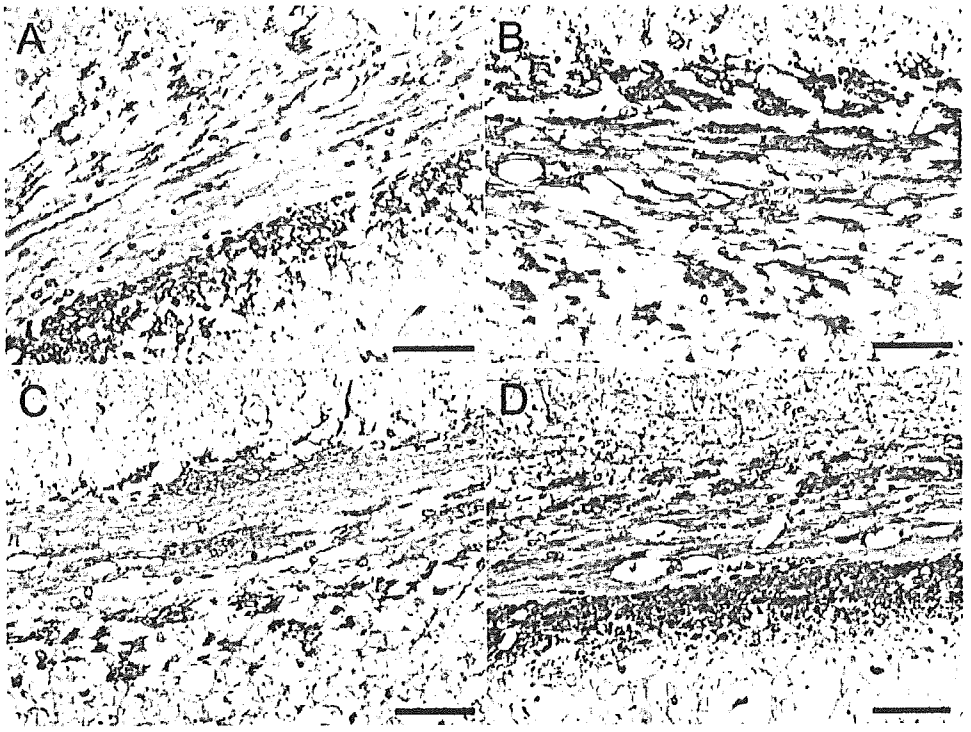

Figure 6: Immunostaining for myelinated fibers of the external capsule of the brains at days 8 (A), 17 (B) and 29 (C) following inoculation of 1×10^9 particles (2.6×10^7 pfu) of adenovirus encoding β-gal, or 8 days after the inoculation of 1×10^8 viral particles (D). The number of myelinated fibers decreased and the remaining fibers appeared fragmented at days 8 (A), 17 (B) and 29 (C) following inoculation of 1×10^9 viral particles (2.6×10^7 pfu). Bar=50 μm

injected into a single mouse brain site resulted in acute, dose-dependent, inflammation, which was reversible within 30 days, and was accompanied with very limited cytotoxicity. However, injection of 1×10^9 pfu resulted in massive cytotoxicity and chronic unremitting inflammation[36].

In contrast to intraparenchymal inoculation, histological studies on the gene transfer into ependymal cells have been limited (*Table 1*). Most of these studies used a recombinant adenovirus as the vehicle for gene transfer. Viral particle doses varied between 1.2×10^6 and 1×10^{10} pfu. The peak time of gene expression varied between days 1 and 9, except for the studies by Davidson *et al.* and Ghodsi *et al.*[16,37]. Ghodsi *et al.* did not mention the difference in immune response in the brain between intraparenchymal and intraventricular inoculation of the virus. Davidson *et al.* only traced the expression of the marker gene in the olfactory bulb after intraventricular inoculation of the virus.

Driesse *et al.* reported the histology of monkey brains, in which recombinant adenovirus encoding the herpes simplex virus-conjugated thymidine kinase gene was injected into the lateral ventricle as a suicide gene therapy. The monkeys did not show any clinical symptoms, but $CD4^+$ T cells, $CD8^+$ T cells and B ($CD19^+$) lymphocytes, plasma cells and histiocytic cells infiltrated the choroid plexus and the superficial layer of the parenchyma resulting in the loss of some ependymal cells at day 21[38]. It was suggested that the intraventricular administration of recombinant virus caused a strong immune response. Because their observations were limited to days 3 and 21 post-administration, they did not observe the expected subsequent brain atrophy.

Here, we show the successful transfer of the β-gal gene into the ependymal layer by the intraventricular inoculation of 1×10^9 particles (2.6×10^7 pfu) of adenovirus. However, β-gal expression rapidly declines and β-gal-positive cells have almost completely disappeared by day 7. Histological examination indicates ventricular dilatation accompanied by diffuse periventricular lymphocytic infiltration, and loss of ependymal cells from the ventricular wall of the brain. The rapid decline of β-gal expression can be easily explained by this loss of ependymal cells. Follow-up MR images showed progressive ventriculomegaly and further histologic analysis revealed edematous changes in the center of the hemisphere, most prominent in the external capsule.

Apoptotic cells were often found in the external capsule of the brain 8 days following inoculation with the high dose of 1×10^9 viral particles. These apoptotic cells are likely to be oligodendrocytes because of their linear arrangement in the external capsule and because their cytoplasm was not positive for GFAP. Immunostaining for MBP showed a clear decrease and fragmentation of myelinated fibers of the external capsule of the brain inoculated with 1×10^9 particles, which was associated with proliferation of astrocytes in the external capsule.

Astrocytes produce various cytokines such as tumor necrosis factor following viral infection[39]. In contrast,

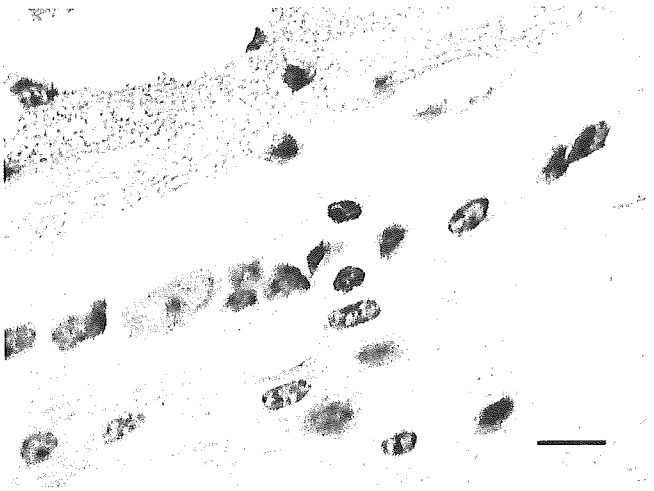

Figure 7: Immunostaining for single-stranded DNA 8 days following inoculation of 1×10^9 particles (2.6×10^7 pfu) of adenovirus encoding β-gal, showing two immunoreactive nuclei in the external capsule of the cerebrum. Bar=10 μm

neurons and oligodendrocytes are sensitive to the effects of the inflammatory cytokines and reactive oxygen species, which are released during an inflammatory response, and Wallerian degeneration is regulated by some inflammatory cytokines[40,41]. These inflammatory cytokines also stimulate the proliferation of reactive astrocytes[42]. Our observations are consistent with these reports.

Thus, the immune response following intraventricular administration of recombinant adenovirus appears to be different from the immune response to intraparenchymal administration of the virus. Normal brain has dendritic cells in the choroid plexus and meninges[43]. The antigen presenting cells in the CSF space would play an important role in inducing the stronger immune response of the CNS, when the virus is injected into the CSF space. Further research is required to elucidate the underlying mechanism of the differences in immune response between the CSF and parenchyma.

Care must be taken when considering that the observed ventriculomegaly depended upon brain

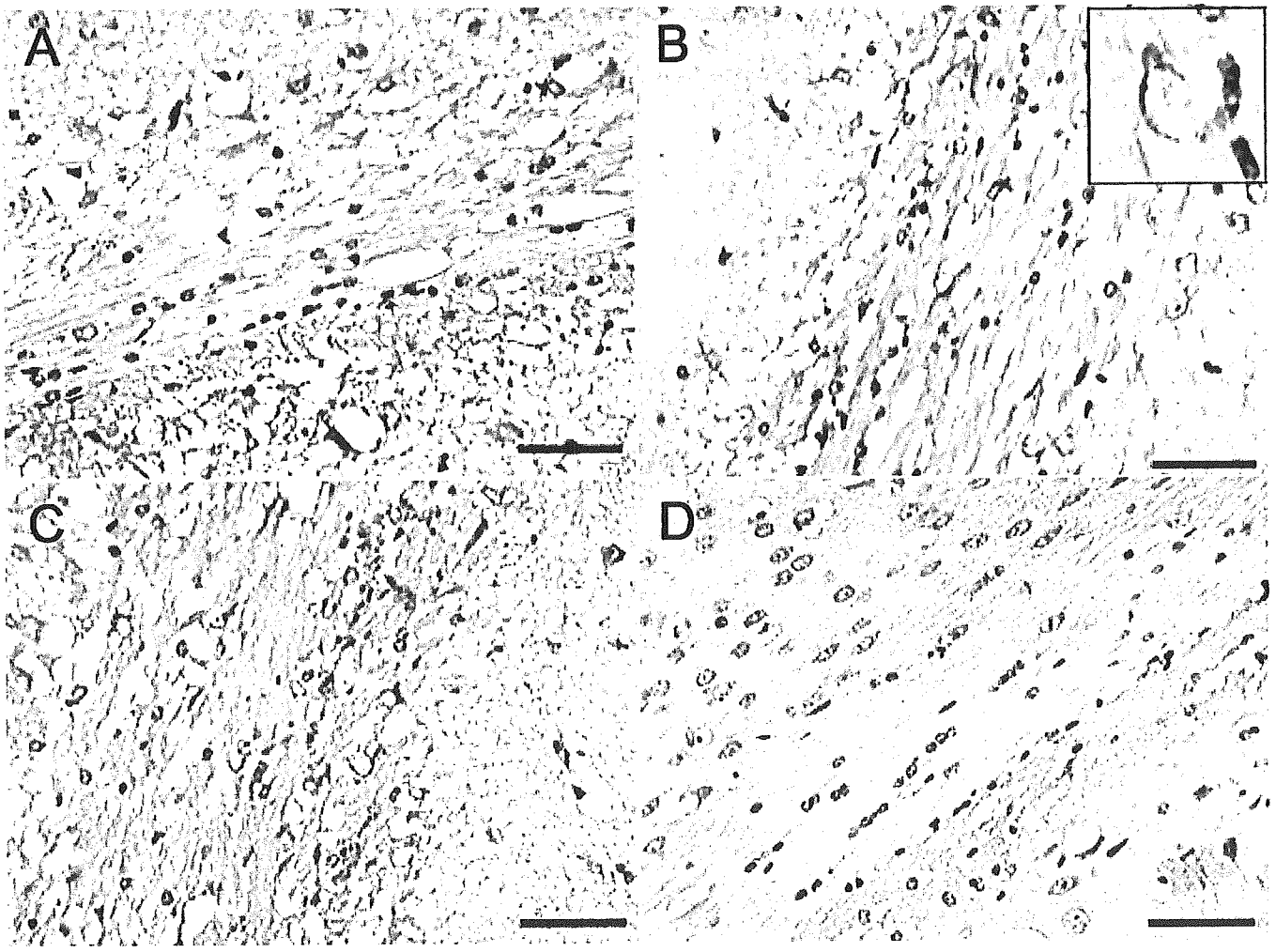

Figure 8: Immunostaining for GFAP of the external capsule of the brains at days 8 (A), 17 (B) and 29 (C) following inoculation of 1×10^9 particles (2.6×10^7 pfu) of adenovirus encoding β-gal and 8 days after the inoculation of 1×10^8 viral particles (2.6×10^6 pfu) (D). Only a few GFAP-positive cells were observed in the external capsule 8 days after the inoculation of 1×10^9 and 1×10^7 viral particles. However, the cytoplasm of the cells with large clear nuclei that proliferated in the external capsule 17 and 29 days after the inoculation were found to be GFAP-positive. Bar=50 μm. The magnified corner in (B) indicates the GFAP-positive cell with a large nucleus

Table 1: List of previous gene transfer to the central nervous system with virus

	Year	Authors	Virus	No. of injected particles	Injecting site	Animals	Peak time (days)	Observation period (days)	Gene
1	1993	Bajocchi *et al.*	Ad	5×10^9 pfu	LV	SD rat	4	6	βgal
2	1995	Ooboshi *et al.*	Ad	1×10^9 pfu	CM	SD rat	1	7	βgal
3	1995	Betz *et al.*	Ad	Particle 1×10^9 pfu	LV	Rat	5	5	βgal
5	1998	Kitagawa *et al.*	Ad	2.5×10^9 pfu	LV	Gerbil	1	21	βgal
6	1998	Yang *et al.*	Ad	1×10^9 particle	LV	CD-1 mice	5	5	βgal
7	1998	Ghodsi *et al.*	Ad	2×10^7 pfu	LV CM	C57BL/6 mice	21	21	βgal
8	1998	Abe *et al.*	Ad	2.5×10^9 pfu	LV	Gerbil	7	21	βgal
9	2000	Davidson *et al.*	AAV	3×10^{10} pfu	LV	C57BL/6 mice	21	105	βgal
10	2000	Yagi *et al.*	Ad	Ad 5×10^7 pfu	LV	Gerbil	2, 4, 7	7	βgal
11	2000	Mao *et al.*	Ad	Unknown	LV	CD-1 mice	5	5	βgal
12	2002	Baekelandt *et al.*	HIV-1	Unknown	LV	Mice	Unknown	Unknown	GFP
13	2002	Lin *et al.*	Ad	1×10^7 pfu	LV	LE rat	3	3	GFP
14	2003	Matsuoka *et al.*	Ad	2×10^8 pfu	LV	Gerbil	2	7	βgal
15	2003	Shirakura *et al.*	SeV	1×10^9 pfu	LV	Gerbil	4	7	GFP
16	2000	Driesse *et al.*	Ad	7.4×10^9 pfu	LV	Monkey	(–)	21	(–)
17	2000	Driesse *et al.*	Ad	5×10^9 pfu	LV	Rat	(–)	16	(–)
18	2000	Muzzin *et al.*	Ad	3×10^8 pfu	LV	Zucker	Rat	9	GFP

Ad=adenovirus, pfu=plaque forming units, LV=lateral ventricle, β-gal=β-galactosidease, GFP=green fluorescent protein, CM=cisterna magna, AAV=adenoassociated virus; HIV-1=human immunodeficiency virus, SeV=Sendai virus.

atrophy or hydrocephalus. Hydrocephalus in humans is often accompanied by periventricular lucency, indicating that the destruction of the ependymal layer permits influx of CSF from the ventricle to the brain parenchyma[44]. In our study, we observed edematous changes in the center of the hemisphere, but degenerative changes were apparent in the external capsule. Therefore, we speculate that the ventricles were compensatory dilated after degeneration of the neural fibers.

In conclusion, it is important to take this diffuse encephalo-ventriculitis into consideration for the clinical application of gene transfer into the ependymal cells or subarachnoid space.

ACKNOWLEDGEMENTS

This study was supported in part by Research Grants (15390433) from the Ministry of Education, Culture, Sports, Science and Technology of Japan.

REFERENCES

1 Wright JL, Merchant RE. Blood-brain barrier changes following intracerebral injection of human recombinant tumor necrosis factor-alpha in the rat. *J Neurooncol* 1994; **20**: 17–25
2 Kern MA, Bamborschke S, Nekic M, *et al.* Concentrations of hepatocyte growth factor in cerebrospinal fluid under normal and different pathological conditions. *Cytokine* 2001; **14**: 170–176
3 Pan W, Kastin AJ. Interactions of cytokines with the blood-brain barrier: Implications for feeding. *Curr Pharm Des* 2003; **9**: 827–831
4 Baker D, Hankey DJ. Gene therapy in autoimmune, demyelinating disease of the central nervous system. *Gene Ther* 2003; **10**: 844–853
5 Ooboshi H, Welsh MJ, Rios CD, *et al.* Adenovirus-mediated gene transfer in vivo to cerebral blood vessels and perivascular tissue. *Circ Res* 1995; **77**: 7–13
6 Viola JJ, Ram Z, Walbridge S, *et al.* Adenovirally mediated gene transfer into experimental solid brain tumors and leptomeningeal cancer cells. *J Neurosurg* 1995; **82**: 70–76
7 Shimamura M, Sato N, Oshima K, *et al.* Novel therapeutic strategy to treat brain ischemia: Overexpression of hepatocyte growth factor gene reduced ischemic injury without cerebral edema in rat model. *Circulation* 2004; **109**: 424–431
8 Le Gal La Salle G, Robert JJ, Berrard S, *et al.* An adenovirus vector for gene transfer into neurons and glia in the brain. *Science* 1993; **259**: 988–990
9 Breakefield XO. Gene delivery into the brain using virus vectors. *Nature Genet* 1993; **3**: 187–189
10 Bajocchi G, Feldman SH, Crystal RG, *et al.* Direct in vivo gene transfer to ependymal cells in the central nervous system using recombinant adenovirus vectors. *Nature Genet* 1993; **3**: 229–234
11 Yoon SO, Lois C, Alvirez M, *et al.* Adenovirus-mediated gene delivery into neuronal precursors of the adult mouse brain. *Proc Natl Acad Sci USA* 1996; **93**: 11974–11979
12 Kitagawa H, Setoguchi Y, Fukuchi Y, *et al.* DNA fragmentation and HSP72 gene expression by adenovirus-mediated gene transfer in postischemic gerbil hippocampus and ventricle. *Metab Brain Dis* 1998; **13**: 211–223
13 Yang GY, Liu XH, Kadoya C, *et al.* Attenuation of ischemic inflammatory response in mouse brain using an adenoviral vector to induce overexpression of interleukin-1 receptor antagonist. *J Cereb Blood Flow Metab* 1998; **18**: 840–847
14 Abe K, Kitagawa H, Setoguchi Y. Temporal profile of adenovirus-mediated *E. coli* lacZ gene expression in normal and post-ischemic gerbil hippocampus and ventricle. *Neurol Res* 1998; **20**: 689–696
15 Driesse MJ, Kros JM, Avezaat CJ, *et al.* Distribution of recombinant adenovirus in the cerebrospinal fluid of nonhuman primates. *Hum Gene Ther* 1999; **10**: 2347–2354
16 Davidson BL, Stein CS, Heth JA, *et al.* Recombinant adeno-associated virus type 2, 4, and 5 vectors: Transduction of variant cell types and regions in the mammalian central nervous system. *Proc Natl Acad Sci USA* 2000; **97**: 3428–3432
17 Yagi T, Maeda M, Tanaka A, *et al.* Detection of the exogenous hGDNF in gerbils under the treatment with AxCAhGDNF adenoviral vector. *Brain Res Brain Res Protoc* 2001; **8**: 88–98
18 Lin H, Lin TN, Cheung WM, *et al.* Cyclooxygenase-1 and bicistronic cyclooxygenase-1/prostacyclin synthase gene transfer protect against ischemic cerebral infarction. *Circulation* 2002; **105**: 1962–1969
19 Shirakura M, Fukumura M, Inoue M, *et al.* Sendai virus vector-mediated gene transfer of glial cell line-derived neurotrophic factor prevents delayed neuronal death after transient global ischemia in gerbils. *Exp Anim* 2003; **52**: 119–127

20 Matsuoka N, Nozaki K, Takagi Y, *et al.* Adenovirus-mediated gene transfer of fibroblast growth factor-2 increases BrdU-positive cells after forebrain ischemia in gerbils. *Stroke* 2003; **34**: 1519–1525
21 Zeimet AG, Marth C. Why did p53 gene therapy fail in ovarian cancer? *Lancet Oncol* 2003; **4**: 415–422
22 Rainov NG, Ren H. Gene therapy for human malignant brain tumors. *Cancer J* 2003; **9**: 180–188
23 Dai Y, Schwarz EM, Gu D, *et al.* Cellular and humoral immune responses to adenoviral vectors containing factor IX gene: Tolerization of factor IX and vector antigens allows for long-term expression. *Proc Natl Acad Sci USA* 1995; **92**: 1401–1405
24 Ohmoto Y, Wood MJ, Charlton HM, *et al.* Variation in the immune response to adenoviral vectors in the brain: Influence of mouse strain, environmental conditions and priming. *Gene Ther* 1999; **6**: 471–481
25 Akli S, Caillaud C, Vigne E, *et al.* Transfer of a foreign gene into the brain using adenovirus vectors. *Nature Genet* 1993; **3**: 224–228
26 Davidson BL, Allen ED, Kozarsky KF, *et al.* A model system for in vivo gene transfer into the central nervous system using an adenoviral vector. *Nature Genet* 1993; **3**: 219–223
27 Dewey RA, Morrissey G, Cowsill CM, *et al.* Chronic brain inflammation and persistent herpes simplex virus 1 thymidine kinase expression in survivors of syngeneic glioma treated by adenovirus-mediated gene therapy: implications for clinical trials. *Nat Med* 1999; **5**: 1256–1263
28 Kielian T, Hickey WF. Inflammatory thoughts about glioma gene therapy. *Nat Med* 1999; **5**: 1237–1238
29 Principles of Laboratory Animal Care formulated by the National Society for Medical Research
30 Guide for the Care and Use of Laboratory Animals prepared by the Institute of Laboratory Animal Resource. NIH Publication No. 86-23, revised 1985
31 Chen SH, Chen XH, Wang Y, *et al.* Combination gene therapy for liver metastasis of colon carcinoma in vivo. *Proc Natl Acad Sci USA* 1995; **92**: 2577–2581
32 Terazaki Y, Yano S, Yuge K, *et al.* An optimal therapeutic expression level is crucial for suicide gene therapy for hepatic metastatic cancer in mice. *Hepatology* 2003; **37**: 155–163
33 Cruz JI, Loste JM, Burzaco OH. Observations on the use of medetomidine/ketamine and its reversal with atipamezole for chemical restraint in the mouse. *Lab Anim* 1998; **32**: 18–22
34 Byrnes AP, Rusby JE, Wood MJ, *et al.* Adenovirus gene transfer causes inflammation in the brain. *Neuroscience* 1995; **66**: 1015–1024
35 Perry VH, Andersson PB, Gordon S. Macrophages and inflammation in the central nervous system. *Trends Neurosci* 1993; **16**: 268–273
36 Lowenstein PR, Castro MG. Inflammation and adaptive immune responses to adenoviral vectors injected into the brain: Peculiarities, mechanisms, and consequences. *Gene Ther* 2003; **10**: 946–954
37 Ghodsi A, Stein C, Derksen T, *et al.* Extensive beta-glucuronidase activity in murine central nervous system after adenovirus-mediated gene transfer to brain. *Hum Gene Ther* 1998; **9**: 2331–2340
38 Driesse MJ, Esandi MC, Kros JM, *et al.* Intra-CSF administered recombinant adenovirus causes an immune response-mediated toxicity. *Gene Ther* 2000; **7**: 1401–1409
39 Lieberman AP, Pitha PM, Shin HS, *et al.* Production of tumor necrosis factor and other cytokines by astrocytes stimulated with lipopolysaccharide or a neurotropic virus. *Proc Natl Acad Sci USA* 1989; **86**: 6348–6352
40 Selmaj K, Raine CS, Farooq M, *et al.* Cytokine cytotoxicity against oligodendrocytes. Apoptosis induced by lymphotoxin. *J Immunol* 1991; **147**: 1522–1529
41 Shamash S, Reichert F, Rotshenker S. The cytokine network of Wallerian degeneration: Tumor necrosis factor-alpha, interleukin-1alpha, and interleukin-1beta. *J Neurosci* 2002; **22**: 3052–3060
42 Selmaj KW, Farooq M, Norton WT, *et al.* Proliferation of astrocytes in vitro in response to cytokines. A primary role for tumor necrosis factor. *J Immunol* 1990; **144**: 129–135
43 McMenamin PG. Distribution and phenotype of dendritic cells and resident tissue macrophages in the dura mater, leptomeninges, and choroid plexus of the rat brain as demonstrated in wholemount preparations. *J Comp Neurol* 1999; **405**: 553–562
44 Serdar M. Periventricular lucency on computed tomography associated with hydrocephalus: What is the cause? *Surg Neurol* 1995; **44**: 285–286

(10)

Postinfarction Gene Therapy Against Transforming Growth Factor-β Signal Modulates Infarct Tissue Dynamics and Attenuates Left Ventricular Remodeling and Heart Failure

Hideshi Okada, MD; Genzou Takemura, MD, PhD; Ken-ichiro Kosai, MD, PhD; Yiwen Li, MD, PhD; Tomoyuki Takahashi, PhD; Masayasu Esaki, MD; Kentaro Yuge, MD, PhD; Shusaku Miyata, MD; Rumi Maruyama, BS; Atsushi Mikami, MD, PhD; Shinya Minatoguchi, MD, PhD; Takako Fujiwara, MD, PhD; Hisayoshi Fujiwara, MD, PhD

Background—Fibrosis and progressive failure are prominent pathophysiological features of hearts after myocardial infarction (MI). We examined the effects of inhibiting transforming growth factor-β (TGF-β) signaling on post-MI cardiac fibrosis and ventricular remodeling and function.

Methods and Results—MI was induced in mice by left coronary artery ligation. An adenovirus harboring soluble TGF-β type II receptor (Ad.CAG-sTβRII), a competitive inhibitor of TGF-β, was then injected into the hindlimb muscles on day 3 after MI (control, Ad.CAG-LacZ). Post-MI survival was significantly improved among sTβRII-treated mice (96% versus control at 71%), which also showed a significant attenuation of ventricular dilatation and improved function 4 weeks after MI. At the same time, histological analysis showed reduced fibrous tissue formation. Although MI size did not differ in the 2 groups, MI thickness was greater and circumference was smaller in the sTβRII-treated group; within the infarcted area, α-smooth muscle actin–positive cells were abundant, which might have contributed to infarct contraction. Apoptosis among myofibroblasts in granulation tissue during the subacute stage (10 days after MI) was less frequent in the sTβRII-treated group, and sTβRII directly inhibited Fas-induced apoptosis in cultured myofibroblasts. Finally, treatment of MI-bearing mice with sTβRII was ineffective if started during the chronic stage (4 weeks after MI).

Conclusions—Postinfarction gene therapy aimed at suppressing TGF-β signaling mitigates cardiac remodeling by affecting cardiac fibrosis and infarct tissue dynamics (apoptosis inhibition and infarct contraction). This suggests that such therapy may represent a new approach to the treatment of post-MI heart failure, applicable during the subacute stage. ***(Circulation.* 2005;111:-.)**

Key Words: heart failure ■ gene therapy ■ myocardial infarction ■ transforming growth factors

Myocardial infarction (MI) often leads to left ventricular (LV) remodeling, which is characterized by ventricular dilatation, diminished cardiac performance, and poor recovery of function.[1] Thus, patients who escape death during the acute stage of a large MI are at high risk of developing heart failure during the chronic stage. Indeed, patients with postinfarction heart failure account for nearly half of the candidates for cardiac transplantation.[2] The extent of the cardiomyocyte death during the acute stage of MI is a critical determinant of the subsequent ventricular remodeling and eventual heart failure, but the complex process of cardiac remodeling is not determined solely by that; hypertrophic responses occur in cardiomyocytes in the surviving portion of the ventricle, followed by ventricular dilatation due to architectural rearrangement of the cardiomyocytes and interstitial cells making up the myocardium.[3–5] In that regard, myocardial fibrosis is one of the most characteristic structural changes in infarcted hearts and contributes to both systolic and diastolic dysfunction.[6,7]

See p 2260

Several lines of evidence point to the critical role played by transforming growth factor-β (TGF-β) during the progression of myocardial fibrosis: (1) TGF-β1 induces increases in both the production and secretion of collagen, increases the abundance of collagen type I and III mRNA in cultured rat cardiac fibroblasts, and stimulates the expression of extracellular matrix proteins in vivo[8]; (2) in vivo gene transfer of TGF-β1 can induce myocardial fibrosis[8]; (3) expression of TGF-β is markedly increased in both infarcted and noninfarcted areas

Received August 11, 2004; revision received January 4, 2005; accepted January 6, 2005.

From the Second Department of Internal Medicine (H.O., G.T., Y.L., M.E., S. Miyata, R.M., S. Minatoguchi, H.F.) and Department of Gene Therapy and Regenerative Medicine (K.K., T.T., K.Y., A.M.), Gifu University School of Medicine, Gifu; and Department of Food Science, Kyoto Women's University, Kyoto (T.F.), Japan.

Correspondence to Hisayoshi Fujiwara, MD, PhD, Second Department of Internal Medicine, Gifu University School of Medicine, 1-1 Yanagido, Gifu 501-1194, Japan. E-mail gifuim-gif@umin.ac.jp

Circulation **is available at http://www.circulationaha.org** **DOI: 10.1161/01.CIR.0000165066.71481.8E**

of hearts after MI[9,10]; and (4) TGF-β is associated with angiotensin II–mediated fibrosis, whereas inhibition of angiotensin II signaling mitigates post-MI cardiac remodeling and improves function.[11,12] Collectively, these findings suggest strongly that TGF-β plays a critical role during the healing process after MI and thus affects cardiac remodeling and function during the chronic stage.

Soluble TGF-β type II receptor (sTβRII) inhibits the action of TGF-β, most likely by adsorbing TGF-β or by acting as a dominant negative receptor.[13] In the present study we hypothesized that postinfarction treatment with sTβRII would mitigate chronic heart failure by affecting the LV remodeling process. We therefore constructed a recombinant adenoviral vector expressing the extracellular domain of the TGF-β type II receptor fused to human immunoglobulin Fc and started its transduction into mouse hindlimbs (systemic transfection) on the third day after MI, a time when therapy would not affect acute ischemic death of cardiomyocytes. We then examined the effects on LV structure and function during the chronic stage of MI and sought possible mechanisms responsible for our observations made both in vitro and in vivo.

Methods

Replication-Defective Recombinant Adenoviral Vectors

A replication-defective adenoviral vector, Ad-TβRIIEx-Fc, which expresses the extracellular domain of the type II TGF-β receptor[13] fused to the Fc portion of human IgG1 under the transcriptional control of cytomegalovirus immediate early enhancer and a modified chicken β-actin promoter, was constructed by in vitro ligation as previously described.[14] Likewise, control Ad-LacZ was prepared as previously described.[15,16]

Measurement of sTβIIR in Plasma

Plasma concentrations of sTβRII after adenoviral transfection were measured in mice (n=5) by detecting human IgG-Fc with the use of an enzyme-linked immunosorbent assay (Institute of Immunology).

Experimental Protocols

The study was approved by our institutional animal research committee. MI was induced in 10-week-old male C57BL/6J mice (Chubu Kagaku, Nagoya, Japan) by ligating the left coronary artery as previously described.[14] In sham-operated mice, the suture was passed but not tied. Ad.CAG-sTβRII (1×10^{11} particles per mouse) was then injected into the hindlimb muscles of the mice. As a control, adenovirus harboring the LacZ gene (Ad.CMV-LacZ) was injected in the same manner.

Protocol 1 (Treatment at Subacute Stage)

MI was induced in 75 mice. Of those, 55 survived to the third day after MI and were entered into the study. They were then randomly assigned into sTβRII (n=27) and LacZ (n=28) treatment groups and were followed up for 4 weeks after MI. Fifteen sham-operated mice were subjected to either of the treatments (LacZ, n=7; sTβRII, n=8) and similarly assessed. In another experiment, on the third day after MI, 10 mice were divided into sTβRII and LacZ treatment groups (n=5 each), and the survivors (n=4 in the sTβRII group and n=3 in the LacZ group) were euthanized on day 10 after MI.

Protocol 2 (In Vitro Experiment)

MI was induced in mice, and 10 days later cardiac myofibroblasts were obtained from the infarcted areas of the hearts according to the method previously described with modification.[16] Briefly, the heart was resected, and the infarcted area was removed. The tissue was then minced and incubated with collagenase type II (Worthington) in Krebs-Ringer buffer for 30 minutes at 37°C. The dissociated cells were plated on 10-cm dishes for 1 hour and then rigorously washed with buffer. The attached remaining nonmyocytes were cultured in DMEM supplemented with 5% mouse serum, which was obtained from mice 7 days after transfection with Ad.CAG-TβRII or Ad.CMG-LacZ. The cells were used for experimentation during the second and third passages. More than 90% of the cells were found to be α-smooth muscle actin (SMA) positive. A mixture of agonistic anti-Fas antibody (1 μg/mL; Pharmingen) and actinomycin D (0.05 μg/mL; Sigma) was applied for 24 hours to induce apoptosis.[17]

Protocol 3 (Treatment at Chronic Stage)

MI was induced in 33 mice that were subsequently observed for 4 weeks with no treatment. At that time, scarring was well established in the infarcts of the 25 surviving mice, and gene treatment with LacZ (n=11) or sTβRII (n=14) was started. These mice were then examined after an additional 4 weeks (8 weeks after MI). In another set of animals, we evaluated sTβRII in the 5-week-old infarcted area (1 week after viral injection) by Western blot using LacZ gene– and sTβRII gene–treated hearts (n=3 each). This was to confirm accessibility of sTβRII into scar tissue.

Physiological Studies

Echocardiograms were recorded 4 weeks after MI with the use of an echocardiographic system (Aloka) equipped with a 7.5-MHz imaging transducer. The right carotid artery was then cannulated with a micromanometer-tipped catheter (SPR 407, Millar Instruments) that advanced into the left ventricle via the aorta for recording pressures and $\pm$dP/dt.

Histological Analysis

After the physiological analyses, all surviving mice were euthanized, and their hearts were removed. The excised hearts were cut into 2 transverse slices; the basal specimens were fixed in 10% buffered formalin and embedded in paraffin, after which 4-μm-thick sections were stained with hematoxylin-eosin, Masson's trichrome, and Sirius red F3BA (0.1% solution in saturated aqueous picric acid) (Aldrich).[14] Quantitative assessments of cell size, cell population, and fibrotic area were performed on 20 randomly chosen high-power fields (HPF) in each section with the use of a LUZEX F multipurpose color image processor (Nireco). Quantitative assessments of cardiomyocyte size (as the transverse diameter), cell population, vessel population, and fibrotic area were performed on 20 randomly chosen HPF in each section with a LUZEX F multipurpose color image processor (Nireco). The number of cardiomyocytes evaluated was 198$\pm$12 cells per heart. Vessels were identified as the lumens outlined by Flk-1–positive endothelial cells on the Flk-1–immunostained sections.

Immunohistochemical Analysis

Deparaffinized 4-μm-thick sections or cultured cells were incubated with primary antibody against α-SMA (Sigma), Flk-1 (Santa Cruz), or pan-leukocyte antigen (CD45, Pharmingen), after which they were immunostained with diaminobenzidine hydrochloride or labeled with immunofluorescent Alexa Fluor 488 or 568 (Molecular Probes). Nuclei were stained with hematoxylin or Hoechst 33342.

Apoptosis was evaluated with the use of the in situ terminal deoxynucleotidyl transferase–mediated nick-end labeling (TUNEL) method with an ApopTag kit (Intergene) as previously described.[14]

For double immunofluorescence, tissue sections or cells were stained first with the use of an FITC-conjugated ApopTag kit (Integene) and then with anti–α-SMA or anti–Flk-1 followed by labeling with Alexa Fluor 568.

Western Blotting

Proteins (100 μg) extracted from hearts in protocol 1 were subjected to 14% polyacrylamide gel electrophoresis and then transferred onto polyvinylidene difluoride membranes. The membranes were then probed with the primary antibody against matrix metalloproteinase-2 (MMP-2) (Daiichi Fine Chemical Co) or atrial natriuretic peptide (ANP) (Santa Cruz).

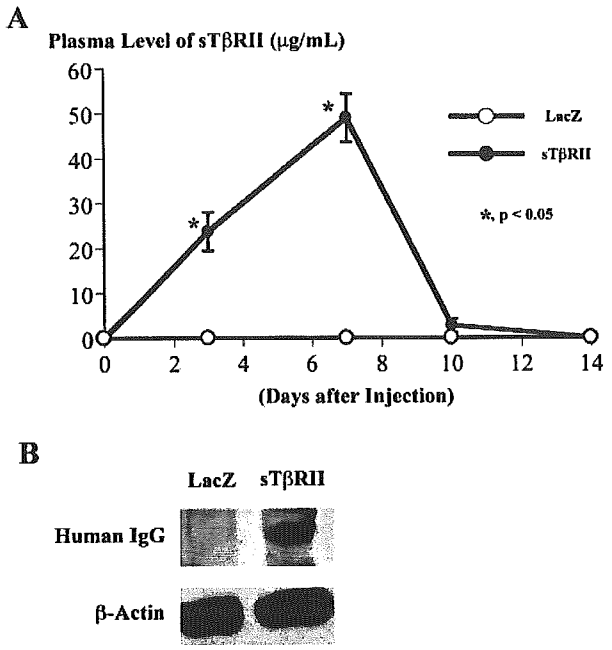

Figure 1. A, Time courses of changes in sTβRII levels measured by enzyme-linked immunosorbent assay in plasma from mice transfected with the LacZ or sTβRII gene. B, Expression of sTβRII protein in infarcted tissues as detected by anti-human IgG.

Infarct tissues were subjected to Western blotting for sTβRII by anti-human IgG antibody (DAKO).

The blots were visualized by means of chemiluminescence (ELC, Amersham), and the signals were quantified by densitometry. β-Actin (analyzed with antibody from Sigma) was the loading control.

Statistical Analysis

Values are shown as mean±SEM. Survival was analyzed by the Kaplan-Meier method with the log-rank Cox-Mantel method. The significance of differences was evaluated with Student *t* tests. Values of $P<0.05$ were considered significant.

Results

Plasma Levels of Exogenous sTβRII

Among mice receiving sTβRII gene transfection, the plasma levels of exogenous sTβRII reached 23.7±4.3 and 49.0±5.4 μg/mL, respectively, 3 and 7 days after the injection (6 and 10 days after MI, respectively), a time when the infarcted area was composed of granulation tissue (Figure 1A). Levels declined steeply thereafter, and sTβRII was undetectable in the plasma 2 weeks after MI. No sTβRII was detected in the LacZ-treated mice at any time. Accessibility of sTβRII into scar tissue was confirmed by Western blotting (Figure 1B). All sham-operated mice survived until 4 weeks after surgery.

Effect of Anti–TGF-β Treatment at Subacute Stage (Protocol 1)

Four Weeks After MI

The survival rate was significantly higher among sTβRII-treated mice than among LacZ-treated control mice 4 weeks after MI (Figure 2A): 26 of 27 mice (96%) in the sTβRII-treated group survived versus 20 of 28 mice (71%) in the control group ($P<0.05$).

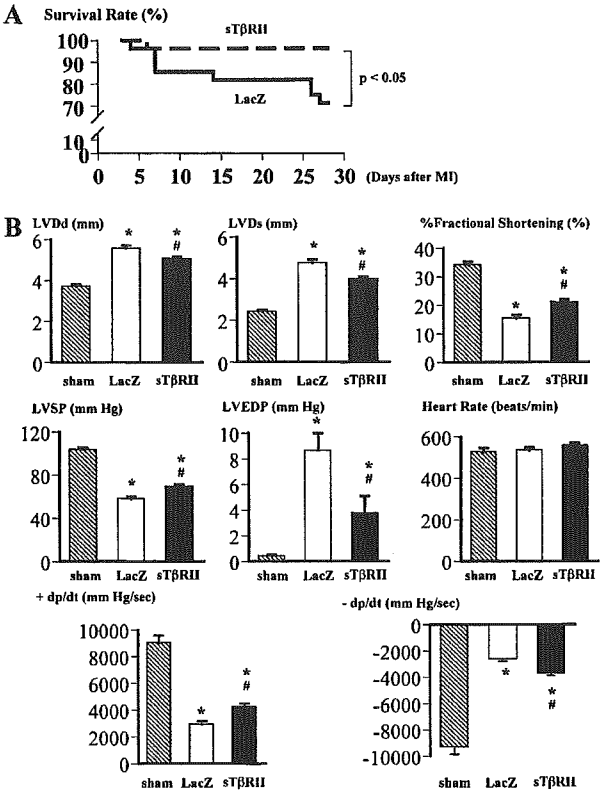

Figure 2. Survival, LV geometry, and LV function during the chronic stage (4 weeks after MI) in MI-bearing mice receiving gene therapy on day 3 after MI. A, Post-MI survival curves for LacZ-treated and sTβRII-treated mice. B to G, Effects of sTβRII therapy on cardiac anatomy and function 4 weeks after MI. LVDd and LVDs indicate left ventricular end-diastolic and end-systolic diameter, respectively; LVSP and LVEDP, left ventricular peak systolic and end-diastolic pressure, respectively; sham, sham-operated control group with LacZ gene treatment. *$P<0.05$, significant difference compared with sham; #$P<0.05$, significant difference compared with the LacZ-treated MI group.

Echocardiography and cardiac catheterization performed 4 weeks after MI showed control mice to have severe LV remodeling with marked enlargement of the LV cavity and signs of reduced cardiac function compared with the sham-operated mice (Figure 2B): decreased LV percent fractional shortening and ±dP/dt and increased LV end-diastolic pressure. These parameters were all attenuated in sTβRII-treated mice (Figure 2B), indicating mitigation of postinfarct remodeling and improved cardiac function. In the sham-operated mice, there was no significant difference in cardiac function 4 weeks after surgery between the sTβRII gene– and LacZ gene–treated group, indicating a negligible effect of sTβRII treatment on cardiac function of sham-operated mice (data not shown).

There was no significant difference in heart weights (Lac Z, 166±9 mg versus sTβRII, 168±6 mg) or in ratios of heart weight to body weight (Lac Z, 6±0.2 mg/g versus sTβRII, 6±0.3 mg/g) between the groups. Although hearts from LacZ-treated mice showed marked LV dilatation with a thin

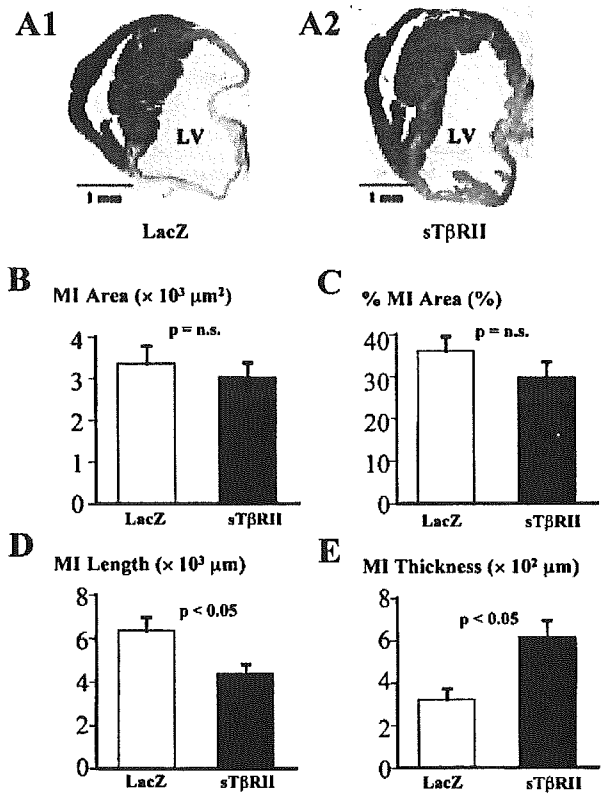

Figure 3. Morphometry of mouse hearts 4 weeks after MI. A, Transverse sections of hearts from mice treated with LacZ (A1) or sTβRII (A2). The sections are stained with Masson's trichrome. Note the smaller LV cavity, shorter infarct segment, and thicker infarct wall in the post-MI heart treated with sTβRII compared with the control heart. B, Absolute area of infarct. C, Percent area of left ventricle taken up by infarct. D, Thickness of infarct. E, Circumferential length of infarct segment.

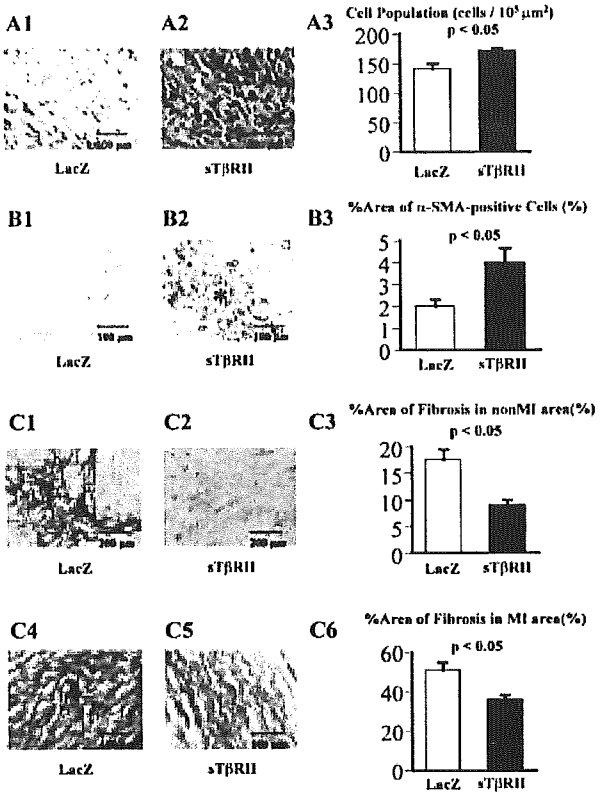

Figure 4. Histological and immunohistochemical preparations from mouse hearts collected 4 weeks after MI. A, Infarcted areas in hearts from LacZ-treated (A1) and sTβRII-treated (A2) mice; graph shows cell density (A3). Sections are stained with hematoxylin-eosin. B, Immunohistochemical analysis of α-SMA within infarcted areas of LacZ-treated (B1) and sTβRII-treated (B2) mice; graph shows percentage of infarcted area taken up by α-SMA–positive cells (B3). Asterisk in B2 indicates a bundle of α-SMA–positive cells. C, Sirius red–stained preparations of noninfarcted (C1 and C2) and infarcted (C4 and C5) areas in LacZ-treated (C1 and C4) and sTβRII-treated (C2 and C5) mice; graphs show percentage of noninfarcted (C3) and infarcted (C6) areas taken up by collagen fibers.

infarcted segment 4 weeks after MI, those from sTβRII-treated mice presented smaller LV cavities (Figure 3A1 and 3A2). Both the absolute area of the infarct and the percentage of the whole LV area taken up by the infarct were comparable between the LacZ- and sTβRII-treated mice (Figure 3B and 3C). On the other hand, the circumferential length of the infarcted segment was shorter and the infarct was thicker in the sTβRII-treated mice (Figure 3D and 3E).

By 4 weeks after MI, the infarcted areas of LacZ-treated mice had been replaced by fibrous scar tissue (Figure 4A1). The infarcts of sTβRII-treated mice, by contrast, contained not only collagen fibers but also numerous cells (Figure 4A2). The noncardiomyocyte population in the infarcted areas was significantly greater in the sTβRII-treated mice (Figure 4A3), as was the percent infarcted area taken up by extravascular α-SMA–positive cells (Figure 4B1 to 4B3). Some α-SMA–positive cells accumulated and formed bundles to run parallel with the infarct wall circumference (Figure 4B2) that were not observed in the infarcted LV walls of the control mice. Still, the population of vessels was comparable in the 2 groups (LacZ, 7.2±0.7 vessels per HPF versus sTβRII, 6.9±0.8 vessels per HPF; P=NS). There was no significant difference in population of CD45-positive cells between the control (0.9±0.1 cells per HPF) and sTβRII-treated hearts (0.8±0.2 cells per HPF; P=NS). The amount of fibrosis assessed in Sirius red–stained sections was significantly reduced in the noninfarcted LV walls and in the infarct region of the sTβRII-treated mice (Figure 4C1 to 4C6). MMP-2 in hearts with 4-week-old MI was greater in hearts with MI compared with the sham-operated hearts, but it was not significantly affected by the sTβRII treatment (Figure 5A and 5B), suggesting a negligible association of the gelatinase activity with sTβRII-induced antifibrosis in the present experimental setting. In addition, the transverse diameters of cardiomyocytes in the noninfarcted areas were significantly greater in the LacZ-treated (17.7±0.3 μm) than in the sTβRII-treated (15.1±0.3 μm) mice (Figure 5C), suggesting that the compensatory cardiomyocyte hypertrophy was more developed in the control mice. Consistent with this finding, Western blot analysis revealed reduced ANP expression in the sTβRII-treated hearts (Figure 5A and 5B).

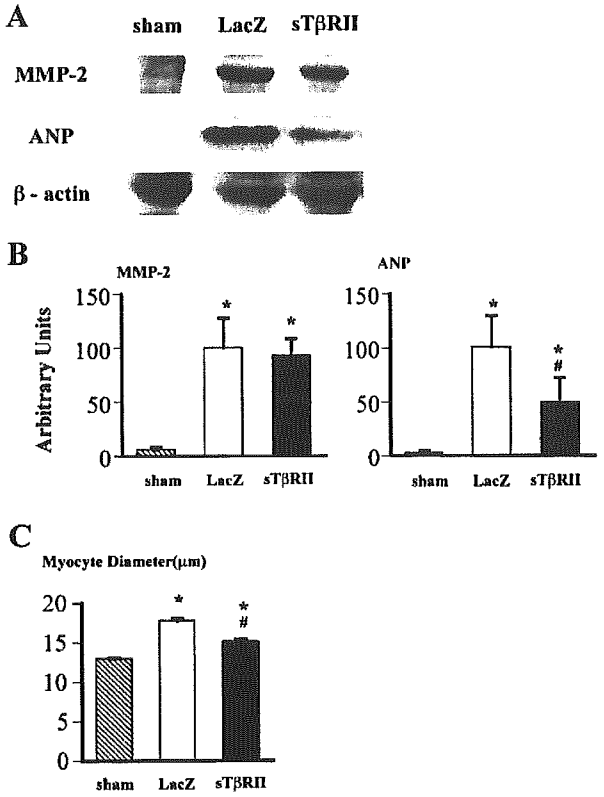

Figure 5. A, Western blotting for MMP-2 and ANP of sham-operated heart and hearts with 4-week-old MI. B, Densitometry of MMP-2 (left) and ANP (right). C, Cardiomyocyte size in sham-operated control hearts and hearts with 4-week-old MI. *$P<0.05$, significant difference compared with sham; #$P<0.05$, significant difference compared with the LacZ-treated MI group.

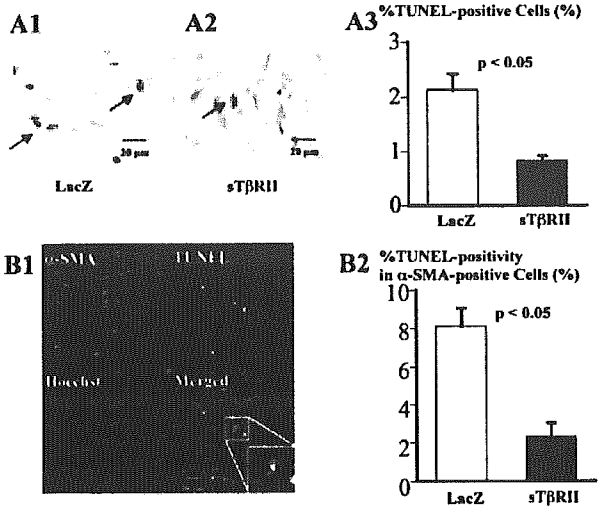

Figure 6. Apoptosis within infarcted tissue 10 days after MI. A, TUNEL-stained preparations from LacZ-treated (A1) and sTβRII-treated (A2) mice. A3, Percentage of TUNEL-positive nonmyocytes within the infarcted area. Arrows indicate positive cells. B, Infarcted tissue obtained from LacZ-treated mice (B1) was double stained with TUNEL and α-SMA immunohistochemistry and observed under a confocal microscope. B2, Percentage of TUNEL-positive cells among the α-SMA–positive cells.

Ten Days After MI

By 10 days after MI, the infarcted areas were composed of granulation tissue, and TUNEL assays indicated that apoptosis was ongoing in both the LacZ- and sTβRII-treated groups. However, the incidence of TUNEL-positive cells was significantly smaller in the sTβRII-treated than in the LacZ-treated group (Figure 6A1 to 6A3). Moreover, double-immunofluorescence assays (TUNEL followed by anti–Flk-1 or anti–SMA antibody) revealed that within the sTβRII-treated group, the incidence of apoptosis was reduced among myofibroblasts/smooth muscle cells (Figure 6B1 and 6B2) but not among endothelial cells (LacZ, 3.5±0.5% versus sTβRII, 3.5±0.2%; P=NS), which suggests that sTβRII may specifically inhibit apoptosis among myofibroblasts. TUNEL-positive cardiomyocytes were extremely rare (<0.01%) in both groups.

Effect of sTβRII on Fas-Induced Apoptosis In Vitro (Protocol 2)

Myofibroblasts obtained from the infarcted areas of mouse hearts 10 days after MI were cultured in medium containing 5% serum collected from LacZ- or sTβRII-treated mice. When the cells were then subjected to Fas-induced apoptosis[16] for 24 hours, the incidence of TUNEL-positive myofibroblasts was significantly lower among cells cultured with sTβRII-containing serum (16±2.9%) than among those cultured with normal serum (43±5.2%; $P<0.05$) (Figure 7). However, such an apoptosis-inhibitory effect by sTβRII-containing serum was completely canceled by an addition of TGF-β1 at the concentration of 1 μg/mL (Figure 7). These findings suggest that sTβRII exerts a direct antiapoptotic effect on cardiac myofibroblasts.

Effect of Anti–TGF-β Treatment at Chronic Stage (Protocol 3)

Using protocol 3, we determined the extent to which inhibiting apoptosis among granulation tissue cells is responsible for the beneficial effects on post-MI heart failure. For this purpose, the sTβRII gene therapy was started at a more chronic stage of MI, after the granulation tissue had already been replaced with scar tissue. The sTβRII (n=14) or LacZ (n=11) gene was delivered to mice 4 weeks after MI, and the mice were examined after an additional 4 weeks (8 weeks after MI). Accessibility of sTβRII into scar tissue was confirmed by Western blotting (Figure 1B). One of 14 sTβRII-treated mice and none of the 11 LacZ-treated mice died during the additional 4-week follow-up (P=NS). This time we found no difference in ventricular geometry or function between the sTβRII-treated and LacZ-treated groups (Table), clearly indicating that the preventive effect of sTβRII gene therapy on heart failure is attributable to its action on granulation tissue during the subacute stage of MI.

Discussion

The present study revealed that postinfarction sTβRII gene therapy, begun at the subacute stage of MI, alleviated adverse remodeling and improved function of the LV during the chronic stage. In addition, we provide novel insights into the

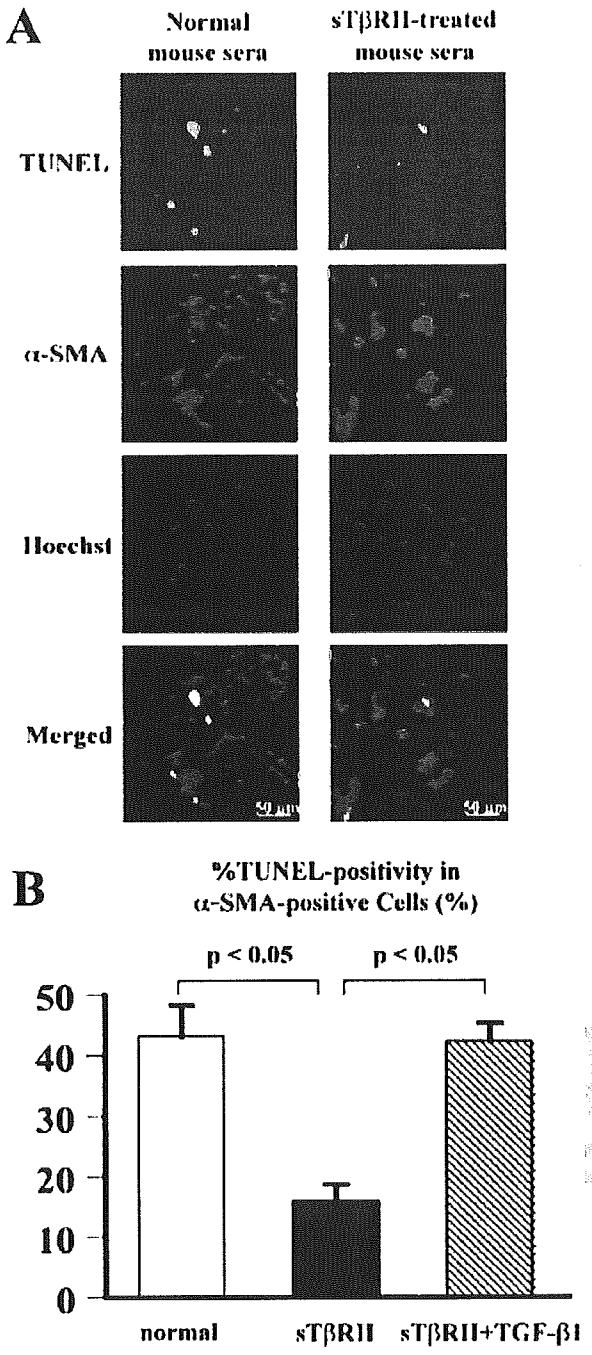

Figure 7. Effect of sTβRII-containing sera on Fas-induced apoptosis among cultured nonmyocytes obtained from the infarcted tissue of hearts 10 days after MI (protocol 2). Confocal micrographs (A) show TUNEL-positive/α-SMA–positive cultured cells. B, Percentage of apoptotic myofibroblasts.

mechanism of the beneficial effect of the TGF-β signal inhibition.

Mechanisms of Beneficial Effects of sTβRII on Postinfarction Heart Failure

The mechanisms responsible for the beneficial effects of inhibiting TGF-β signaling on post-MI heart failure appear somewhat complicated, probably reflecting the multiple biological effects of TGF-β. TGF-β signaling acts as a strong inducer of extracellular matrix and as an immunomodulator of chemotaxis by fibroblasts and inflammatory cells.[18–20] In the infarcted heart, TGF-β expression is regulated by locally generated angiotensin II via angiotensin II type 1 receptor binding, and angiotensin-converting enzyme inhibitors and angiotensin II type 1 receptor blockade attenuated postinfarction ventricular remodeling equally.[11,12] However, the manner in which direct inhibition of TGF-β signaling in the infarcted heart affects the postinfarction process has not been well elucidated . In the present study inhibition of TGF-β signaling by exogenous sTβRII significantly reduced cardiac fibrosis, confirming the fibrogenetic effect of TGF-β on post-MI hearts. Because myocardial fibrosis contributes to both systolic and diastolic dysfunction in the heart,[6,7] reducing it by inhibiting TGF-β signaling is one way in which to mitigate LV remodeling and heart failure. MMP-2 activity seemed to be not significantly associated with sTβRII-induced antifibrosis in the present experimental setting.

Perhaps the most notable finding of the present study is the effect of anti–TGF-β therapy on infarct geometry, ie, the shortening of the infarcted segment and the thickening of the infarcted wall, without a change in absolute infarcted area. Contraction of the infarcted tissue likely contributes to suppression of LV dilatation. Because wall stress is proportional to the cavity diameter and inversely proportional to the wall thickness (Laplace's law)[21] and because wall stress and adverse LV remodeling (dilatation) have a vicious relationship, accelerating one another, it is easy to surmise that such an alteration in the geometry of the infarct would markedly improve the hemodynamic state of the heart.

Ventricular Geometry, Function, and Histology 8 Weeks After MI Among Mice Transfected With the Indicated Gene 4 Weeks After MI (Protocol 3)

	LacZ (n=11)	sTβRII (n=13)	*P*
LVED diameter, mm	6.0±0.1	6.3±0.2	0.11
% Fractional shortening	16.7±0.6	16.1±0.6	0.53
Heart rate, bpm	502±21	544±20	0.16
LVSP, mm Hg	85±3	80±3	0.21
LVEDP, mm Hg	9±1	9±1	0.84
+dP/dt, mm Hg/s	3847±101	3608±150	0.22
−dP/dt, mm Hg/s	−3642±166	−3337±144	0.18
MI area, $\times 10^3$ μm^2	2.1±0.2	2.4±0.3	0.53
% MI area	21.5±3.2	24.2±3.0	0.57
MI segmental length, $\times 10^3$ μm	6.1±0.9	6.4±0.7	0.78
MI wall thickness, $\times 10^2$ μm	2.4±0.4	2.0±0.2	0.43
% Fibrosis in non-MI area	17.7±1.8	18.1±1.9	0.88
% Fibrosis in MI area	50.6±3.6	51.5±3.9	0.56
Cell population in MI area, cells/10^5 μm^2	149±6	144±5	0.56
Area of α-SMA–positive cells, %	1.9±0.9	2.0±0.2	0.75

LVED indicates LV end-diastolic; LVSP, LV peak systolic pressure; and LVEDP, LV end-diastolic pressure.

Inhibition of TGF-β signaling also qualitatively altered the infarct tissue. We found an increased abundance of α-SMA–positive cells (myofibroblasts and smooth muscle cells) in the extravascular area of infarcts in sTβRII-treated hearts. Those cells are well known to play an important role in wound contraction during the healing process,[22] and to then disappear via apoptosis.[23,24] Recently, we reported that blockade of myofibroblast apoptosis by the treatment with pan-caspase inhibitor or with soluble Fas, a competitive inhibitor of Fas, attenuates postinfarction ventricular remodeling and heart failure.[25,26] We speculate that the preserved myofibroblasts may contribute structurally to the thickening of the infarct scar. In addition, although the property of contractile function of these myofibroblasts has not been elucidated, it is conceivable that contractile myofibroblasts that are running parallel with the infarct circumference may shrink the infarct into coronal directions and increase the infarct thickness.

It is thus notable that sTβRII had a direct inhibitory effect on apoptosis among myofibroblasts in granulation tissue, both in vivo and in vitro. This is consistent with the report by Hagimoto et al,[27] who showed that TGF-β1 sensitizes pulmonary epithelial cells to Fas-induced apoptosis. Conversely, TGF-β is known to promote transdifferentiation of fibroblasts into myofibroblasts,[28] ie, inhibition of TGF-β signaling possibly results in reduction of myofibroblast population. Inhibition of TGF-β signaling thus appears to have reciprocal effects on myofibroblast population: its reduction through interfering with transdifferentiation from fibroblasts and its augmentation through blocking apoptotic death. In the present experimental setting, the gene product peaked during the granulation tissue phase (1-week-old infarct) when myofibroblasts were already abundant but their apoptosis was ongoing. In the 4-week-old infarct tissue, however, naturally occurring apoptosis was already complete in the control MI hearts. These findings may explain our data that the population of α-SMA–positive cells was balanced to gain in the post-MI scar tissue of the TGF-β signal–inhibited hearts. Taken together, these findings suggest that myofibroblasts escaping apoptosis may survive even during the chronic stage of MI, accumulate, form bundles, and contribute to infarct contraction. In addition, this mechanism appears critical for functional improvement, as transfection of the sTβRII gene was ineffective if started during the chronic stage of MI, when most α-SMA–positive cells have already disappeared (see protocol 3 above).

Because in the present study sTβRII gene therapy was started on the third day after MI, it is unlikely that it influenced cardiomyocyte apoptosis during the acute stage. It is also unlikely that this therapy affected cardiomyocyte survival by inhibiting apoptosis at the subacute or chronic stages. This is because, in contrast to an earlier report,[4] we found that apoptosis was negligible among cardiomyocytes at any stage of MI.

Time Window Within Which to Inhibit TGF-β Signaling

TGF-β signaling is believed to have cardioprotective effect during ischemia/reperfusion, perhaps as a result of inhibition of tumor necrosis factor-α release, improvement of endothelium-dependent relaxation, prevention of reactive oxygen species generation, and/or inhibition of upregulation of matrix metalloproteinase-1.[29,30] For these reasons, inhibition of TGF-β signaling during the acute stage of MI is considered harmful. In addition, our data indicate that late inhibition of TGF-β signaling (during the scar phase of MI) is without effect. It thus appears that there is a therapeutic time window that is critical for inhibition of TGF-β signaling to elicit the beneficial effects on post-MI heart failure.

Limitations and Clinical Implications

There is considerable evidence indicating that the TGF-β signal exerts a protective effect against atherosclerosis in mouse models by preventing lipid lesion formation.[31–33] This potential limitation might have to be taken into account in application of the anti–TGF-β strategy.

Rapid recanalization of the occluded coronary artery is presently the best clinical approach to the treatment of acute MI; if performed in time, it enables salvage of the ischemic myocardial cells. Unfortunately, most patients miss the chance for coronary reperfusion therapy because to be effective it must be performed within a few hours after the onset of infarction.[34] The present findings suggest that this novel therapeutic strategy may mitigate the chronic progressive heart failure seen in patients after large MIs. When initiated during the subacute stage, inhibition of TGF-β signaling may benefit patients who missed the chance for coronary reperfusion.

Acknowledgments

We thank Akiko Tsujimoto and Hatsue Ohshika for technical assistance.

References

1. Pfeffer MA, Braunwald E. Ventricular remodeling after myocardial infarction: experimental observations and clinical implications. *Circulation.* 1990;81:1161–1172.
2. Hosenpud JD, Bennett LE, Keck BM, Boucek MM, Novick RJ. The Registry of the International Society for Heart and Lung Transplantation: seventeenth official report: 2000. *J Heart Lung Transplant.* 2000;19:909–931.
3. Pfeffer JM, Pfeffer MA, Fletcher PJ, Braunwald E. Progressive ventricular remodeling in rat with myocardial infarction. *Am J Physiol.* 1991;260:H1406–H1414.
4. Cheng W, Kajstura J, Nitahara JA, Li B, Reiss K, Liu Y, Clark WA, Krajewski S, Reed JC, Olivetti G, Anversa P. Programmed myocyte cell death affects the viable myocardium after infarction in rats. *Exp Cell Res.* 1996;226:316–327.
5. Weisman HF, Bush DE, Mannisi JA, Weisfeldt ML, Healy B. Cellular mechanisms of myocardial infarct expansion. *Circulation.* 1988;78:186–201.
6. Burlew BS, Weber KT. Connective tissue and the heart: functional significance and regulatory mechanisms. *Cardiol Clin.* 2000;18:435–442.
7. Jalil JE, Doering CW, Janicki JS, Pick R, Shroff SG, Weber KT. Fibrillar collagen and myocardial stiffness in the intact hypertrophied rat left ventricle. *Circ Res.* 1989;64:1041–1050.
8. Lijnen PJ, Petrov VV, Fagard RH. Induction of cardiac fibrosis by transforming growth factor-beta1. *Mol Genet Metab.* 2000;71:418–435.
9. Hao J, Ju H, Zhao S, Junaid A, Scammell-La Fleur T, Dixon IM. Elevation of expression of Smad2, 3, and 4, decorin and TGF-beta in the chronic phase of myocardial infarct scar healing. *J Mol Cell Cardiol.* 1999;31:667–678.
10. Deten A, Holzl A, Leicht M, Barth W, Zimmer HG. Changes in extracellular matrix and in transforming growth factor beta isoforms after coronary artery ligation in rats. *J Mol Cell Cardiol.* 2001;33:1191–1207.
11. Schieffer B, Wirger A, Meybrunn M, Seitz S, Holtz J, Riede UN, Drexler H. Comparative effects of chronic angiotensin-converting enzyme inhi-

bition and angiotensin II type 1 receptor blockade on cardiac remodeling after myocardial infarction in the rat. *Circulation.* 1994;89:2273–2282.
12. Yu CM, Tipoe GL, Wing-Hon Lai K, Lau CP. Effects of combination of angiotensin-converting enzyme inhibitor and angiotensin receptor antagonist on inflammatory cellular infiltration and myocardial interstitial fibrosis after acute myocardial infarction. *J Am Coll Cardiol.* 2001;38: 1207–1215.
13. Isaka Y, Akagi Y, Ando Y, Tsujie M, Sudo T, Ohno N, Border WA, Noble NA, Kaneda Y, Hori M, Imai E. Gene therapy by transforming growth factor-beta receptor-IgG Fc chimera suppressed extracellular matrix accumulation in experimental glomerulonephritis. *Kidney Int.* 1999;55:465–475.
14. Li Y, Takemura G, Kosai K, Yuge K, Nagano S, Esaki M, Goto K, Takahashi T, Hayakawa K, Koda M, Kawase Y, Maruyama R, Okada H, Minatoguchi S, Mizuguchi H, Fujiwara T, Fujiwara H. Postinfarction treatment with an adenoviral vector expressing hepatocyte growth factor relieves chronic left ventricular remodeling and dysfunction in mice. *Circulation.* 2003;107:2499–2506.
15. Chen SH, Chen XH, Wang Y, Kosai K, Finegold MJ, Rich SS, Woo SL. Combination gene therapy for liver metastasis of colon carcinoma in vivo. *Proc Natl Acad Sci U S A.* 1995;92:2577–2581.
16. Katwa LC, Campbell SE, Tyagi SC, Lee SJ, Cicila GT, Weber KT. Cultured myofibroblasts generate angiotensin peptides de novo. *J Mol Cell Cardiol.* 1997;29:1375–1386.
17. Ni R, Tomita Y, Matsuda K, Ichihara A, Ishimura K, Ogasawara J, Nagata S. Fas-mediated apoptosis in primary cultured mouse hepatocytes. *Exp Cell Res.* 1994;215:332–337.
18. Moses HL, Yang EY, Pietenpol JA. TGF-beta stimulation and inhibition of cell proliferation: new mechanistic insights. *Cell.* 1990;63:245–247.
19. Postlethwaite AE, Keski-Oja J, Moses HL, Kang AH. Stimulation of the chemotactic migration of human fibroblasts by transforming growth factor beta. *J Exp Med.* 1987;165:251–256.
20. Lu L, Chen SS, Zhang JQ, Ramires FJ, Sun Y. Activation of nuclear factor-kappaB and its proinflammatory mediator cascade in the infarcted rat heart. *Biochem Biophys Res Commun.* 2004;321:879–885.
21. Yin FC. Ventricular wall stress. *Circ Res.* 1981;49:829–842.
22. Gabbiani G. The myofibroblast in wound healing and fibrocontractive diseases. *J Pathol.* 2003;200:500–503.
23. Desmouliere A, Redard M, Darby I, Gabbiani G. Apoptosis mediates the decrease in cellularity during the transition between granulation tissue and scar. *Am J Pathol.* 1995;146:56–66.
24. Takemura G, Ohno M, Hayakawa Y, Misao J, Kanoh M, Ohno A, Uno Y, Minatoguchi S, Fujiwara T, Fujiwara H. Role of apoptosis in the disappearance of infiltrated and proliferated interstitial cells after myocardial infarction. *Circ Res.* 1998;82:1130–1138.
25. Hayakawa K, Takemura G, Kanoh M, Li Y, Koda M, Kawase Y, Maruyama R, Okada H, Minatoguchi S, Fujiwara T, Fujiwara H. Inhibition of granulation tissue cell apoptosis during the subacute stage of myocardial infarction improves cardiac remodeling and dysfunction at the chronic stage. *Circulation.* 2003;108:104–109.
26. Li Y, Takemura G, Kosai K, Takahashi T, Okada H, Miyata S, Yuge K, Nagano S, Esaki M, Khai NC, Goto K, Mikami A, Maruyama R, Minatoguchi S, Fujiwara T, Fujiwara H. Critical roles for the Fas/Fas ligand system in postinfarction ventricular remodeling and heart failure. *Circ Res.* 2004;95:627–636.
27. Hagimoto N, Kuwano K, Inoshima I, Yoshimi M, Nakamura N, Fujita M, Maeyama T, Hara N. TGF-beta 1 as an enhancer of Fas-mediated apoptosis of lung epithelial cells. *J Immunol.* 2002;168:6470–6478.
28. Desmouliere A, Geinoz A, Gabbiani F, Gabbiani G. Transforming growth factor-beta 1 induces alpha-smooth muscle actin expression in granulation tissue myofibroblasts and in quiescent and growing cultured fibroblasts. *J Cell Biol.* 1993;122:103–111.
29. Lefer AM, Ma XL, Weyrich AS, Scalia R. Mechanism of the cardioprotective effect of transforming growth factor beta 1 in feline myocardial ischemia and reperfusion. *Proc Natl Acad Sci U S A.* 1993;90: 1018–1022.
30. Chen H, Li D, Saldeen T, Mehta JL. TGF-beta 1 attenuates myocardial ischemia-reperfusion injury via inhibition of upregulation of MMP-1. *Am J Physiol.* 2003;284:H1612–H1617.
31. Grainger DJ. Transforming growth factor beta and atherosclerosis: so far, so good for the protective cytokine hypothesis. *Arterioscler Thromb Vasc Biol.* 2004;24:399–404.
32. Mallat Z, Gojova A, Marchiol-Fournigault C, Esposito B, Kamate C, Merval R, Fradelizi D, Tedgui A. Inhibition of transforming growth factor-beta signaling accelerates atherosclerosis and induces an unstable plaque phenotype in mice. *Circ Res.* 2001;89:930–934.
33. Robertson AK, Rudling M, Zhou X, Gorelik L, Flavell RA, Hansson GK. Disruption of TGF-β signaling in T cells accelerates atherosclerosis. *J Clin Invest.* 2003;112:1342–1350.
34. Reimer KA, Vander Heide RS, Richard VJ. Reperfusion in acute myocardial infarction: effect of timing and modulating factors in experimental models. *Am J Cardiol.* 1993;72:13G–21G.